Title: Mapping one million small reservoirs in Brazil highlights widespread environmental and policy implications

Authors: Kylen Solvik[1,2]*, Yaffa Truelove[1], Jennifer K. Balch[1,3], Michael J. Lathuillière[4], Thiago H. Fontenelle[5], Andréa D. de Almeida Castanho[6], Michael T. Coe[6], Christina Shintani[6], Carlos M. Souza Jr.[7], Marcia N. Macedo[2,6,8,9]

Affiliations:

[1]Department of Geography, University of Colorado Boulder; Boulder, 80309, USA
[2]Department of Ecology, Evolution, and Environmental Biology, Columbia University; New York, 10027, USA
[3]Environmental Data Science and Inclusion Lab (ESIIL), University of Colorado Boulder; Boulder, 80309, USA
[4]Stockholm Environmental Institute; Stockholm, 120 30, Sweden
[5]National Water and Sanitation Agency (ANA); Brasília, 70610-200, Brazil
[6]Woodwell Climate Research Center; Falmouth, 02540, USA
[7]Imazon—Amazonia People and Environment Institute; Belém, 66055-200, Brazil
[8]Columbia Climate School, Columbia University, New York, 10027, USA
[9]Instituto de Pesquisa Ambiental da Amazonia, Brasília, DF, Brazil

*Corresponding author. Email: kylen.solvik@columbia.edu

Abstract: Small dams and reservoirs disrupt hydrological connectivity and increase evaporative water loss across Brazil, yet most remain unmapped. Applying deep learning to Sentinel satellite data from 2021, we created a comprehensive map of 1.1 million small on-stream reservoirs (<50 ha). Their 7,597 km^2 cumulative surface area surpasses the combined area of Brazil's three largest mega-dam impoundments. Especially concentrated in areas with high cattle herd densities and precipitation variability, 78% are found in headwater sub-basins, which are vital for downstream water quality and ecosystem health. The reservoirs lose an extra 4.2 km^{3}yr^{-1} to surface evaporation—equivalent to 29% of total annual urban water use in Brazil. Our findings highlight the overlooked socio-environmental consequences of small reservoirs for land and water management.

Introduction

While large dams have drawn intense scrutiny for their environmental and social consequences, small stream barriers and their impoundments have received relatively little attention from scientists and policymakers despite growing evidence that they are widespread[1,2] and can have lasting cumulative impacts on freshwater ecosystems, water resources, and biogeochemical cycling. Recent research has shown that small dams increase evaporative water losses in agricultural systems[3,4]; raise stream water temperature[5–7]; reduce hydrological connectivity[8,9]; degrade water quality[10,11]; and harm biodiversity[8,12]. These impacts extend beyond the region: small lakes and especially reservoirs are important, though poorly quantified, global sources of methane and carbon dioxide to the atmosphere[13–16]. Global Dam Watch estimates that there are 4 million reservoirs smaller than 1 km^2 with a total surface area of 53,000 km^2 around the world, but most of these remain unmapped[17]. Growing scientific evidence of their cumulative impacts belies an urgent need for coherent, spatially consistent data on the locations and sizes of small reservoirs at continental scales.

In Brazil, where hundreds of thousands of small dams have been constructed in rural landscapes accompanying the expansion of cattle ranching[3], crop irrigation[18], mining[19], and aquaculture[20], improved location and size data for small reservoirs are increasingly needed for environmental compliance and sustainable water governance. While scientists and policymakers have focused on curbing deforestation or on the environmental impacts of mega-dam projects like the Belo Monte hydropower plant[21], small dams have been largely overlooked despite important management implications for water and land. Under the National Water Resources Policy[22], surface water usage permits are granted through basin-scale assessments of existing allocations and flow rates to ensure sustainable management. Despite having critical water balance consequences[3,23], small dams are often missing from these assessments since they frequently lack permits and their locations and sizes are generally unknown. In addition, Brazil's 2012 Forest Code requires that a 15-100m buffer around on-stream reservoirs larger than 1 ha be set aside as Permanent Preservation Areas (APPs)[24]. Since the updated Forest Code came into effect, the Amazon Fund has invested over $30 million USD into state-level projects to manually digitize properties, protected areas, and waterbodies including artificial reservoirs[25], but progress and accuracy vary dramatically across states. Future updates will require continued investment to maintain this massive digitization effort—in Bahia alone almost 2,000 people were trained for the digitization—unless parts of the process can be automated.

Automatically detecting small reservoirs requires a model that can both identify the presence or absence of water (water vs. non-water) and distinguish between types of waterbodies (reservoirs vs. natural lakes)—non-trivial tasks for a human let alone a model. Previous approaches to reservoir mapping have typically focused on large reservoirs to the exclusion of small ones[17,26]; relied on flawed assumptions about the creation and disappearance of reservoirs[27]; mapped point locations instead of full reservoir extents[28–30]; and/or required manual labeling or ground surveys over large areas[1,31].

To fill this methodological gap and meet the growing need for a comprehensive map of small reservoirs in Brazil, we trained and applied a hybrid attention-convolution deep neural network (the "Multi-Scale Attention Network" or MA-Net)[32] semantic segmentation model on Sentinel-1 synthetic aperture radar (SAR) and Sentinel-2 multi-spectral satellite data to accurately and comprehensively delineate the full perimeters of on-stream reservoirs smaller than 50 ha (0.5 km^2) across all of Brazil. Neural networks have been successfully applied to a wide range of remote sensing applications, including water detection[33], urban object segmentation[34], change detection[35], cloud filtering[36], and building identification[37], but until now they have only been applied to small-reservoir segmentation over spatial extents orders-of-magnitude smaller than Brazil[38]. One obstacle has been a lack of high-quality, region-specific training data, which we solved with an extensive effort to manually annotate a total of 4,474 reservoirs in 1,314 randomly selected Sentinel images (5 km x 5 km each).

We used the resulting map to analyze the spatial distribution of small dam creation and quantify some of the hidden risks of excluding small reservoirs from land and water management decisions. First, we modeled reservoir density for each Brazilian municipality using a generalized additive model (GAM) and 11 social, economic, and environmental predictors. Then, we analyzed the distribution of reservoirs by stream order across Brazil's 406,858 Pfafstatter level-8 sub-basins. Next, we used climate data to estimate cumulative evaporative water losses from reservoirs—a crucial impact on the local and regional hydrologic cycle[3,23,39]. Finally, we discuss crucial implications for land and water management under Brazil's National Water Resources Policy and Forest Code, including the total area of native vegetation restoration needed to comply with the Forest Code's reservoir APP requirement.

Results

Deep learning maps over a million small reservoirs

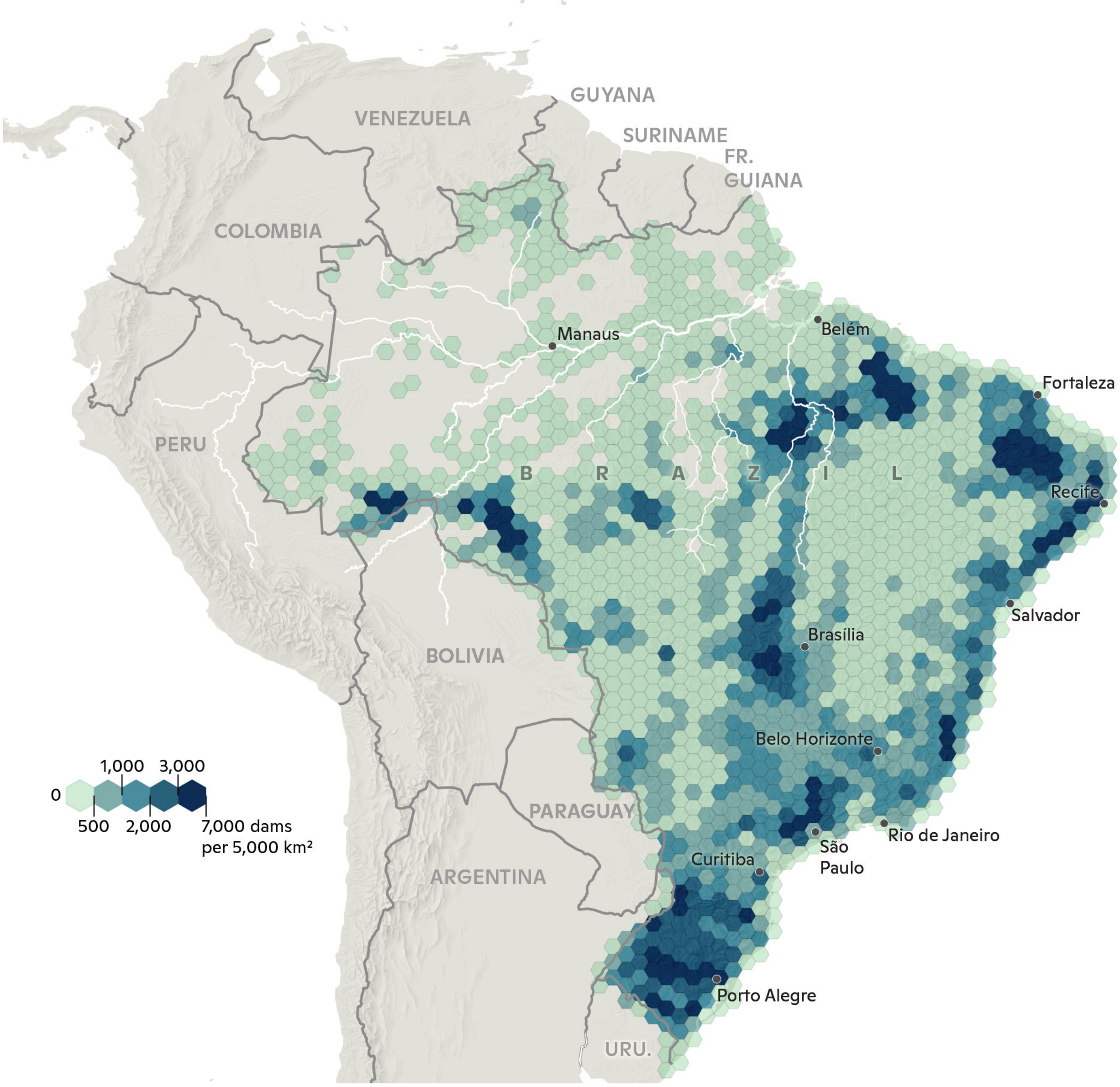

Figure 1. A million small reservoirs detected across Brazil in 2021. Here we display the density of mapped reservoirs as the number present in each 5,000-km^2 hexagon. Trained on 4,474 manually annotated reservoirs, the Multi-Scale Attention Network (MA-Net) model detected and delineated over 1.1 million reservoirs smaller than 50 ha (0.5 km^2) based on data from Sentinel-1 and -2.

Our model mapped 1,126,861 (725,267–1,280,671) small on-stream reservoirs (< 50 ha) in Brazil with a total surface area of 7,597 km^2 (5,072–10,770 km^2; ranges calculated +/- one 10 m pixel around perimeter of each reservoir, see "Methods"), greater than the combined surface area of the three largest hydroelectric reservoirs in Brazil: the Sobradinho, Tucuruí, and Balbina dams (~7,238 km^2 combined)[17]. Since the cloud-free satellite mosaics used for annotation, training, and prediction are biased towards dry-season acquisitions, our reservoir count and area are conservative estimates. The highest reservoir densities occur in pockets of the Pampa biome in the south and the Caatinga in the northeast, areas with long histories of agricultural and—in the Caatinga—drought (Figure 1, Supplementary Figure 1). Recent agricultural frontier regions in the Amazon and Cerrado also have very high concentrations of reservoirs, notably in Goiás and throughout the Amazon's "arc of deforestation", including Rondônia, Acre, Mato Grosso, and the MATOPIBA region. The lowest densities occur in the Pantanal—where natural waterbodies abound to meet surface water needs—and the intact areas of the central Amazon. Supplementary Tables 1-4 include reservoir statistics for each biome, state, macroregion, and hydrographic region.

Our approach consistently identified more reservoirs and greater surface area than previously reported in Brazil (Supplementary Table 5). Despite their large cumulative area, 87% of identified reservoirs were smaller than 1 ha (0.01 km^2). The mean and median surface areas were 0.67 ha (0.67 ha) and 0.21 ha, respectively, making them difficult to detect using lower-resolution sensors. Three existing countrywide datasets include small reservoirs: (a) the official waterbodies dataset from ANA[40]; (b) the Cadastro Ambiental Rural (CAR) data from each state's environmental ministry[41]; and (c) MapBiomas Agua's Landsat-based waterbodies dataset[42]. Compared to the small (<50 ha) artificial waterbodies mapped in each of these datasets, our estimated total surface area and reservoir counts were 35-44% higher and 71–557% higher, respectively. As another point of comparison, our total reservoir count is similar to Europe's estimated 1.2 million total river barriers, calculated by correcting existing dam databases with stream walkover surveys[1].

Overall, the MA-Net model performed well on the challenging task of segmenting on-stream reservoirs (Figure 2, Supplementary Figures 2-3), with a test-set pixel-wise F1-Score of 78.8% (precision = 78.4% and recall = 79.2%; Supplementary Table 6) and a higher object-based precision (77.4%) than recall (61.4%), suggesting that, despite identifying more reservoirs than previous methods, our final reservoir counts are still likely conservative (Supplementary Table 7). Using high-resolution satellite imagery, we manually validated a random sample of 5,000 reservoir detections, 66.1% of which were confirmed true positive detections (Supplementary Table 8).

Accuracy varied across Brazil's diverse landscapes and fluvial systems (Tables S6-8), with the highest accuracy in the Pampa and for reservoirs from 1-10 ha in surface area, and the lowest accuracy in the Pantanal and Mata Atlântica and for reservoirs from 0.05-0.1 ha (0.05 ha, or five Sentinel pixels, was chosen as our lower detection limit based on low accuracy below this threshold). The most common false positives were off-stream artificial reservoirs (72% of false positives in the manually validated set of 5,000 detections) and natural waterbodies (22%), especially in low-relief wetlands such as those in the Pantanal and the lavrado of Roraima where cattle ranching and roads co-occur with numerous and diverse natural water bodies. While wetlands appear particularly challenging for the model, out of all six biomes the Pantanal had the lowest density of reservoirs (0.03 reservoirs per km^2 of land area) and the lowest ratio of reservoirs relative to the count of all known waterbodies in the MapBiomas Água dataset (0.17; Supplementary Table 1), suggesting that overall the model is not indiscriminately mistaking wetland water bodies as reservoirs. Nevertheless, caution should be applied when using this data over wetlands, where there may be more false positives. For small reservoirs, mixed sub-pixels also create uncertainty around the area and, due to our size thresholds, count of reservoirs. To quantify this, we applied binary morphological erosion and dilation, resulting in a total area range of 5,072–10,770 km^2 (67 – 142% of our original estimate) and count range of 725,267 – 1, 280,671 (64 – 114%). See "Methods" for a full description of data processing, modeling, and evaluation.

Figure 2. Reservoir detections (n=1,289) over a 1,000 km^2 region near Santa Maria, Rio Grande do Sul. Where previous approaches to stream barrier mapping have primarily used meter-scale commercial satellite data to identify point locations of dams, our method segments full reservoir boundaries from publicly available Sentinel data by using a hybrid attention-convolution neural network that integrates spectral and object shape information of the reservoir and surrounding context. (**A**) Location of area in southern Brazil, with state outlines shown in black. (**B**) False positive in a river at a bridge crossing. (**C-E**) Correctly identified reservoirs in agricultural landscapes, but the size of largest reservoir in (C) was underestimated. (**F**) False positive water tank (not on-stream) near the town of São Sepé. Basemap: ESRI World Imagery[43].

Small reservoirs are closely linked to agriculture

Throughout Brazil, the detected reservoirs are primarily located in agricultural areas, especially pastureland (Figure 3). Based on the dominant MapBiomas land-use/land-cover (LULC)[44] within a 1 km buffer of each reservoir (see "Methods"), 55.4% of reservoirs occur in pasture (0.40 reservoirs per km^2 of pastureland in Brazil) and 15.4% in cropland (0.28 per km^2 of cropland). Of the remaining 29.2% associated with all other LULC types (0.05 per km^2), three-quarters have at least 10% pasture or cropland within the 1-km buffer. The Amazon and Cerrado, the two biomes with the largest cattle herds[45], have the highest number of reservoirs in pasture. The only biome where more reservoirs occur in cropland than pasture is the Pampa, where croplands are extensive[46] and cattle often graze on native grasslands or in rotation with crops[47]. The Mata Atlântica and Cerrado biomes, which have seen large swaths of pasture converted to cropland in recent years[48], have the next highest proportions of reservoirs in croplands, raising the question of whether reservoirs originally built in pastureland persist in the landscape after conversion to cropland—an important area for future research that could identify opportunities for derelict reservoir removal and stream restoration. The semi-arid, drought-prone Caatinga, where there is a long history of building reservoirs called "*açudes*" to help secure water and produce energy locally[49], is the only biome where a non-agricultural LULC is dominant.

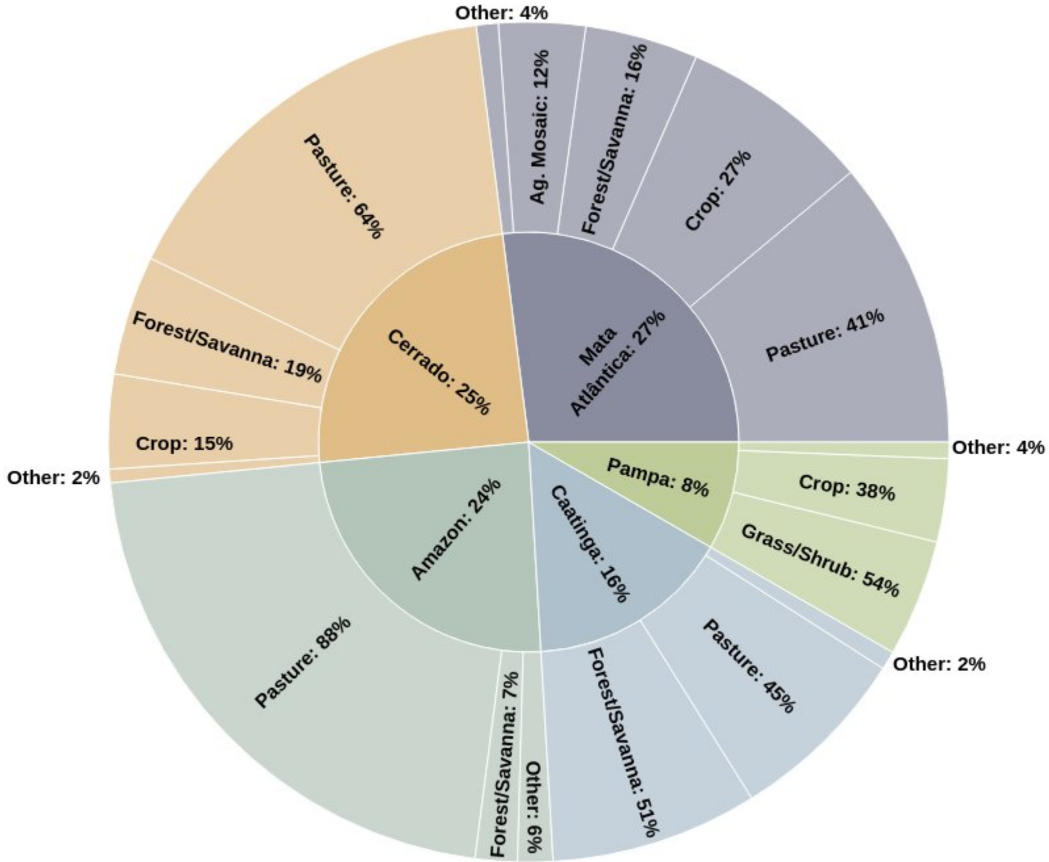

Figure 3. Reservoirs are concentrated in agricultural areas across Brazil. Distribution of the 1,126,861 small reservoirs across Brazilian biomes (inner wedges) and associated land use/cover categories (outer wedges) for 2021. The land-use and land-cover (LULC) classes considered for each biome were: Pasture, Crop, Agricultural Mosaic, Forest/Savanna, Grass/Shrub, and Other. For visualization, we excluded the Pantanal biome (<1% of reservoir detections) and grouped LULC classes comprising <10% of reservoirs in a biome into "Other". Biome boundaries are from the Brazilian Institute of Geography and Statistics (IBGE)[50] and LULC data are from the MapBiomas Collection 10 Land Cover and Land Use dataset[44]**.**

To better understand dam creation and use, we modeled per-municipality reservoir counts using a negative binomial GAM with a log link function and 11 social, environmental, and economic predictor variables (see "Methods"). Model responses were offset using the log of municipality area to control for size variations. The GAM model explained 65.9% of the deviance in reservoir counts between municipalities (Figure 4). All included variables were statistically significant ($p<0.01$) predictors based on a chi-squared test of the fitted splines, but variable importance testing—calculated via hierarchical partitioning to estimate each variable's contribution to the explained deviance—identified cattle herd density as the most important variable (32.8% of the explained deviance), followed by municipality coordinates (21.9%), mean monthly precipitation and standard deviation of monthly precipitation (21.2%), population density (6.0%), road-river intersections (5.6%), biome (3.8%), and proportion of land converted from natural vegetation between 1985 and 2021 (3.7%). The land conversion data is limited to 1985, the start of the MapBiomas data, and so does not account for areas with longer histories of land-conversion for agriculture, limiting its explanatory power. The remaining variables—soy

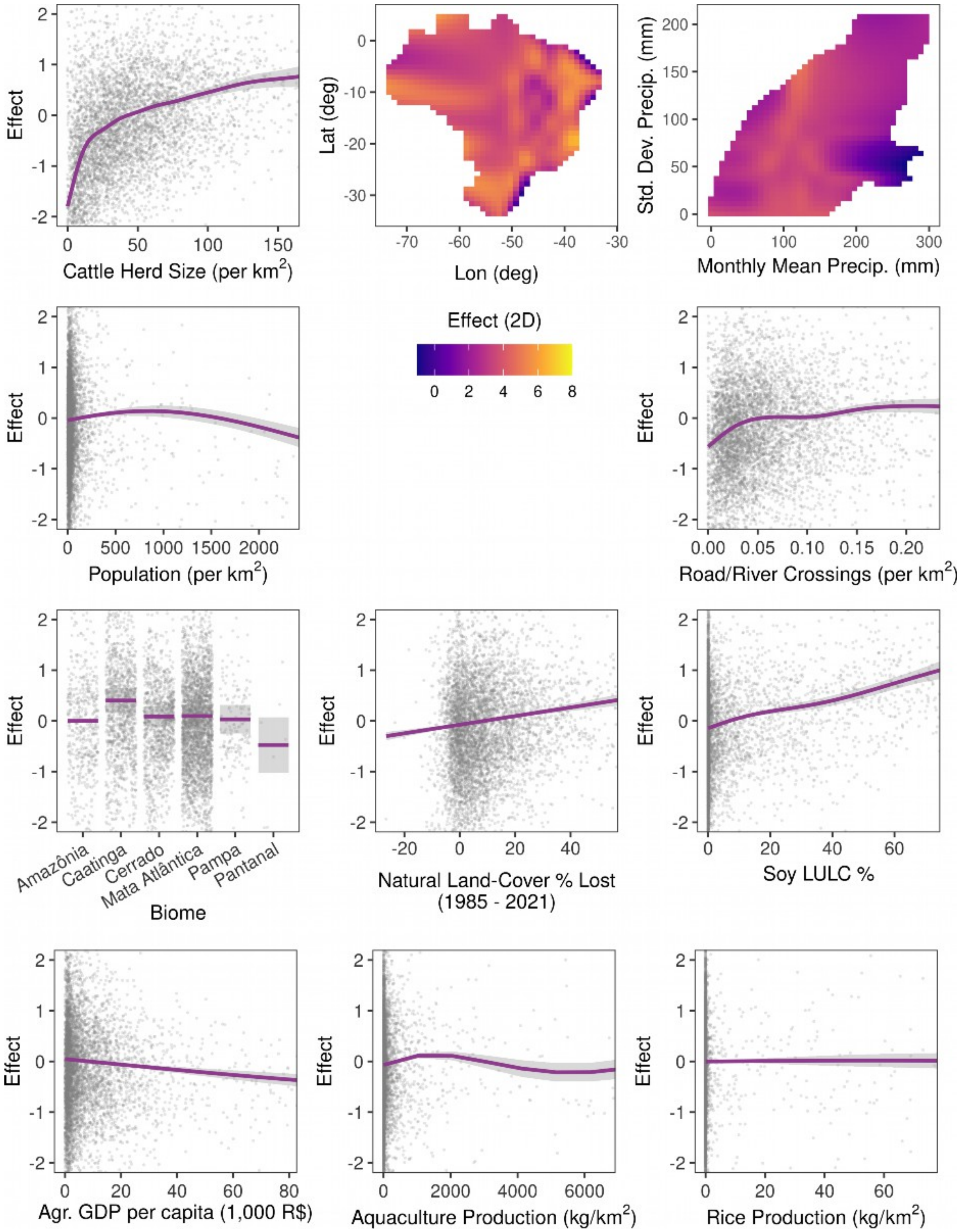

Figure 4. Fitted terms of generalized additive model of per-municipality reservoir count. Variables are ordered (top-left to bottom-right) by contribution to overall explained deviance of the model (65.9%), determined via hierarchical partitioning (Supplementary Table 11). All variables had significant chi-squared tests ($p < 0.01$). Grey shading shows the 95% confidence interval of the spline estimates. For visualization, the x-axis is limited to the 99th percentile of each term, but all values were included in the actual model.

land area, aquaculture production, agricultural GDP per capita, and rice production—had small, but still statistically significant, contributions (Supplementary Table 11). Irrigated land area, which was also tested, was not significant, but this relationship could strengthen in the future as irrigation is projected to increase dramatically in coming years[51].

Although the municipality modeling cannot determine causality, the results underscore the strong spatial correlation between reservoirs and agriculture, particularly cattle ranching. As shown in Figure 4, cattle density has a strong positive effect on reservoir presence, but it appears to saturate moderately above ~50 head per km^2 of municipal land area. Reservoir counts are also higher in municipalities with lower total precipitation and higher precipitation variability, whereas areas with consistent high precipitation throughout the year had lower counts on average. The density of river-road intersections, although limited by incomplete data on road and river networks, also shows a positive relationship that saturates at approximately 0.05 per km^2. Land-clearing and soy area both have weaker but more linear positive relationships to reservoir counts. Like deforestation, small reservoirs are tightly linked to agricultural expansion—particularly cattle ranching, settlement/population growth, and road construction—but have received far less attention, leading to overlooked consequences for freshwater ecosystems and water resources.

Previously unmapped alteration of headwater catchments across Brazil

Overlooking small reservoirs has obscured the alteration of streams across Brazil, particularly in sensitive headwater sub-basins. Nearly one-third (32.3%) of the country's 406,858 Level 8 sub-basins[52] contain at least one reservoir from our dataset, while just 12% contain a known artificial water body from ANA waterbodies dataset and only 0.2% contain a hydroelectric dam[40]. Even more importantly, our detections are particularly concentrated in low-order sub-basins: 878,936 reservoirs (78% of all detections) are located in order 1-3 sub-basins, while just 7,577 are in orders 7-10 (Figure 5). This differs from the hydroelectric dams in ANA's dataset, which are most common in mid-level sub-basins (62% in orders 4-6). The most heavily impacted headwaters are found in the Tocantins-Araguaia (150,553 reservoirs; 85% of all found in the basin), Paraná (142,641; 71%), and Amazon (115,476; 69%) watersheds—all regions with extensive cattle ranching, particularly in the states of Rondônia, Mato Grosso, Goiás, and Mato Grosso do Sul[45].

Understanding the impacts of these dams on stream discharge, habitat connectivity, and groundwater recharge is a vital area for future research, particularly given the high concentration in critical headwater catchments. Where one small dam may cause only minor disruptions, the installation of many consecutive barriers in the same stream or watershed has profound cumulative effects on ecosystem structure and function. By breaking up and slowing the flow of water, small dams reduce hydrological connectivity[9] and increase stream temperatures[5–7]—particularly in the headwaters, where reservoirs replace free-flowing streams typically shaded by adjacent gallery forests with shallow, stagnant waterbodies exposed to direct sunlight. The dams thus disrupt aquatic wildlife movement[12] and reduce downstream water quality for animals and humans alike[10,11]. However, dams in systems with many diverging and meandering stream forms may not have the same fragmentation impacts. In addition to shedding light on the widespread alteration of streams throughout the country, our reservoir map can accelerate research on the differential effects of dams across Brazil's diverse fluvial sys-tems.

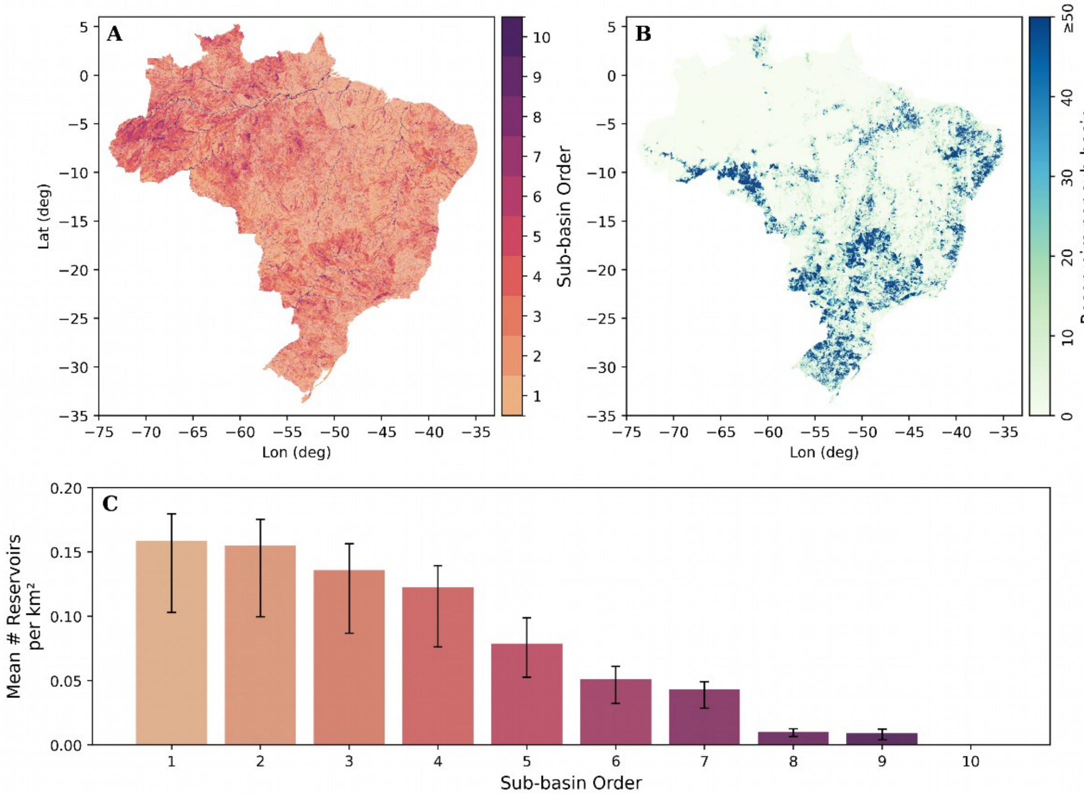

Figure 5. Small reservoirs are highly concentrated in headwater streams. (**A**) Map of Brazil's 406,858 Pfafstetter level-8 sub-basins colored by each sub-basin's max Strahler stream order[52]. (**B**) Reservoir count per level-8 sub-basin. (**C**) Mean reservoir density by sub-basin order. Error bars show results of morphological dilation (upper-bound) and erosion (lower) uncertainty estimation. 78% of all reservoir detections were located in headwater (order 1-3) sub-basins.

Water balance impacts: an extra 4.2 km^3yr^{-1} of evaporative water loss

Although individually small, these reservoirs have important cumulative water balance impacts which have been largely overlooked until now. Using our reservoir map and reference potential evapotranspiration from the Brazil Improved Daily Weather Gridded Data dataset[53], we estimate that small reservoirs lost 10.7 km^3yr^{-1} (7.2 – 15.1 km^3yr^{-1}; based on uncertainty erosion/dilation of the reservoirs) of water to the atmosphere in 2021, a net increase of 4.2 km^3yr^{-1} (2.9 – 5.9 km^3yr^{-1}) over the baseline evapotranspiration if the reservoirs were *not* present (see "Methods"). For comparison, 4.2 km^3yr^{-1} is equivalent to roughly 29% of total urban water use for Brazil, estimated at 14.5 km^3yr^{-1} [39]. This has vital implications for our understanding of basin water balance throughout Brazil. Excluding baseline evapotranspiration, ANA estimated net excess evaporation from reservoirs to account for 27.1 km^3yr^{-1} of water consumption across the country in 2021, the single largest factor besides irrigation[39]. While large reservoirs drive their country-wide estimate (the 12 largest impoundments contribute 58% of the total evaporation), adding our newly identified reservoirs, excluding those which overlap with existing water bodies in the ANA data[40], increased the total evaporative water loss by 2.2 km^3yr^{-1} or 8.6%. Critically, 78% (1.7 km^3yr^{-1}) of this new evaporation came from headwater sub-basins (Pfafstetter level 8 basins with outlet Strahler order 1 – 3), which previously had few mapped reservoirs and where the excess evaporation could be particularly consequential due to lower overall water fluxes. Using reference evapotranspiration instead of open water evaporation, our estimates are likely conservative. Future research, aided by our reservoir maps, should explore constraining them further to better inform water budgets and permitting assessments.

Not all these water balance impacts are necessarily negative. Surface water evaporation from reservoirs may partially offset the decreased evapotranspiration that accompanies large-scale conversion of native vegetation (e.g., forests and savannas) to croplands or pasture[54]. At the farm scale, they can also help retain water that would otherwise be exported quickly downstream, thus potentially mitigating the increased discharge observed in many deforested areas[55,56]. However, in other regions such as northeastern Brazil, dams may inhibit streamflows that are already decreasing due to climate change and water use[57]. Understanding the spatially heterogeneous and complex hydrological impacts of small reservoirs—and how they interact with other influences such as fishing, agrochemical runoff, and land-conversion—is a critical direction for future research, especially as climate change and increasing human demand threaten Brazil's water security[58].

Discussion

Accurately mapping 1,126,861 small reservoirs (< 50 ha) raises important land and water policy implications related to Brazil's National Water Resources Policy and Forest Code. First, our reservoir dataset addresses a major blind spot in water resource management. Without location and size data on small reservoirs, water permitting assessments under the National Water Resource Policy have lacked vital information affecting basin-scale water balance, including a net 4.2 km^3yr^{-1} of evaporative water loss from small impoundments as well as reservoir withdrawals for cattle watering and crop irrigation. While existing permits can be used to approximate withdrawals based on reservoir size, future research—aided by our dataset—should prioritize quantifying these flows to help policymakers and water managers balance the water storage benefits of reservoirs against the reduced water quality and quantity for people, animals, and plants downstream.

Beyond water, the policy implications extend to land management. Brazil's 2012 Forest Code requires that all on-stream reservoirs larger than 1 ha be surrounded by an APP, but many reservoirs were built without permitting and compliance is rarely assessed. Based on a conservative 30 m buffer, only 36.9% of reservoirs larger than 1 ha have natural land-cover covering at least half of their required APP. Meeting the APP requirements for these reservoirs would require restoring native vegetation on 2,370 km^2 of land—a large area, but less than 2% of the 120,000 km^2 Brazil has pledged to restore by 2030 under the Paris Agreement. Prioritizing restoration of the riparian zones around reservoirs would provide a host of ecosystem benefits including improved water quality[59,60] and reduced evaporative water loss[61], helping to offset the negative effects of these dams. Future research should also examine the potential for removal of unused reservoirs and restoration of streams.

Our publicly available reservoir map and annotated training data can help accelerate reservoir research in Brazil and beyond. Whereas previous studies were forced to either focus on limited regions where detailed reservoir information was available[3,23] or approximate reservoir count and surface area using power-law estimates[4], our dataset enables spatially explicit reservoir research that, crucially, accounts for variability across Brazil—a geographically, environmentally, and socially diverse country expecting uneven impacts from climate change[57]. A similar approach could be applied to other parts of the tropics and the world, although it would likely need extensive training data annotation specific to the region-of-interest. Because our method can provide a consistent map of small reservoirs using one year of satellite data, it can also be updated annually to monitor changes and uncover emerging areas of stream damming. In Brazil, while existing reservoirs may shrink as more water is lost to evaporation due to increasing atmospheric water demand, climate change could drive more dam-building to bolster water security, especially if deforestation and cattle production continue to expand. Additionally, the rapid expansion of crop irrigation in Brazil is expected to demand 41% more water withdrawals by 2040[39], which, since irrigation relies primarily on surface water[51], could also drive construction of new reservoirs.

Drawing on advancements in deep learning and satellite data over the past decade, we revealed an important gap in our understanding of the state of freshwater ecosystems by mapping widespread stream damming that has large but previously unseen cumulative impacts on water resources and aquatic ecosystems. As changing precipitation patterns drive communities to develop new strategies to ensure water security[10,62], there is a pressing need for further research on the extent and consequences of small dams worldwide[2]. Global databases of waterbodies provide invaluable information, but they exclude the locations and extents of millions of small dams. As new satellites and methods are developed in the coming years, our framework can be applied to monitor and quantify the impacts and benefits of small reservoirs around the world, unlocking new insights into how humans interact with and alter the environment.

Methods

I. Generating Sentinel-1 and -2 composites

Using Google Earth Engine[63], we created cloud-free mosaics of Sentinel-1 and Sentinel-2 imagery over all of Brazil, excluding outlying islands. First, we selected all scenes collected in 2017 (for model training) and 2021 (for the final map). For Sentinel-2, we recreated the compositing algorithm described in Pekel et al.[64]. We first eliminated all scenes with greater than 50% cloud cover. Then, for each pixel over the entire region, we identified the least cloudy observation from the available scenes based on Google's Sentinel-2 Cloud Score+ dataset[65]. We removed any observations with a cloud score greater than 10% more than that minimum cloud score, leaving a cloud-free stack of observations for each pixel over the entire country. Note that the cloud-filtering process, while necessary, creates a bias towards dry-season imagery when there are fewer clouds but reservoir extents are at their smallest, likely leading to some underestimation of reservoir counts and areas. Finally, we applied top-of-atmosphere correction and calculated the median value from the remaining observations to create a wall-to-wall, cloud-free mosaic of all 10m and 20m bands (Bands 2-8A, 11, and 12). The 20m bands were later resampled to 10m using bilinear interpolation to match the other inputs. Cloud-filtering was not necessary for Sentinel-1 scenes since Synthetic Aperture Radar (SAR) can penetrate clouds. Instead, we created a simple median-value composite of the "VV" and "VH" polarization modes ("HH" and "HV" are only available for polar regions). The final composites were exported from Google Earth Engine, and the rest of the analysis was performed on virtual machines on Google Cloud Platform.

II. Training MA-Net segmentation model

After creating and exporting the Sentinel mosaics, we randomly extracted 500 x 500-pixel (5km x 5km) subsets of the mosaics for manual annotation to create the training dataset (Supplementary Figure 2). Using LabelBox, an online platform for annotating training data[66], we outlined every reservoir in each subset image. The reservoirs were labeled using Sentinel-2 Normalized Difference Water Index (NDWI)[67] as reference and, if needed, higher-resolution satellite imagery available on Google Maps. Two criteria were used for distinguishing on-stream reservoirs from other waterbodies during annotation: (1) Is there a visible dam or other obstruction (e.g., road) impounding the water? This is typically evidenced by an unnaturally straight line on the downstream edge of the waterbody. (2) Is there evidence of a stream path flowing into and/or out of the reservoir? This is usually indicated by a riverine path with higher NDWI than the surroundings, even when the stream is dry. In total, 1,314 images were labeled in this way, containing a total of 4,474 reservoirs. Oxbow lakes and small rivers proved to be particularly challenging for the model to distinguish from reservoirs, and so to provide more training examples for these cases we selected another 190 subsets over river floodplains. These were only used for training and were excluded from the validation and test set. The annotations were exported as masks, where 0 represented a non-reservoir pixel (including land and water) and 1 represented a reservoir pixel. Then the images were split into training, validation, and test sets using a 60%-

20%-20% split. In the end, the training set consisted of 978 images (including the 190 "floodplains" images), and the validation and test sets each contained 263.

During annotation, subset images were presented for labeling in random order. However, there were instances where the human annotator could not accurately and confidently identify the reservoirs in the image. In those cases, that candidate image was skipped. This was unavoidable, but it does introduce a positive bias in our eventual accuracy metrics. In addition, because the project first began with a focus on the Amazon/Cerrado transition zone, this area is overrepresented in the annotated data—53% of the annotated images come from this region, which covers 32% of Brazil's land area.

We evaluated three different convolutional and attention-based neural network architectures: the U-Net convolutional neural network[68], the Segformer attention-based network[69], the hybrid Multi-Scale Attention Network (MA-Net) which adds channel and position-wise self-attention mechanisms to a U-Net-like convolutional network[32]. Implemented in Segmentation Models PyTorch[70], the U-Net and MA-Net were trained with a resnet-34 encoder[71] while the Segformer used the Mix Transformer – B2 encoder[69], all without retrained weights because there are limited pre-trained weights available for the band-combinations used as inputs. For the U-Net and MA-Net, we used the Adam optimizer[72] with a Dice loss function, a learning rate of $1e^{-4}$, dropout of 0.5 applied to the decoder, and an exponential learning rate decay of 0.9 applied after every epoch (one full pass through the training dataset). For the Segformer, we used the same loss function and dropout but followed the original Segformer article's recommendations by using the AdamW optimizer[73] and a learning rate schedule with a linear warmup over the first 200 steps from $2e^{-7}$ to $2e^{-5}$ followed by cosine annealing scheduled from step 200 to 3690 (30 epochs). To prevent overfitting, we stopped training when the validation set's pixel-wise F1-score failed to increase for five epochs in a row.

We experimented with a variety of band combinations: all bands, excluding SAR, and excluding 20-m bands. We also tested adding calculated vegetation and water indices. Based on the validation set F1-score, we found that the best band combination included the four 10m Sentinel-2 bands (blue, green, red, and near-infrared), the two Sentinel-1 SAR bands (corresponding to VV and VH polarization), and four vegetation and water indices: Normalized Difference Vegetation Index (NDVI), McFeeters's Normalized Difference Water Index (NDWI)[67], Gao's NDWI[74], and Modified-NDWI[75]. To provide more context for the neural network, 640 x 640-pixel images were used as inputs and the output masks were clipped to 500 x 500. The training data were augmented by applying random vertical and horizontal flips and random 90-degree rotations, all with 0.5 probability. The model inputs and outputs are visualized in Supplementary Figure 4. The hybrid attention-convolution MA-Net had the highest F1-score on the validation set, and so was selected as the final model for inference (Supplementary Table 7, Supplementary Figure 5).

After training, we tuned the binary prediction threshold on the validation set by evaluating the pixel-wise F1-score at each potential threshold between 0 and 1 by 0.01 increments. A threshold of 0.62 proved the best, and so we used that value for model inference and accuracy assessment (see sections III and IV below). We then computed the object-based precision, recall, and F1-Scores for the validation set overall and at 6 different size classes (below 0.05 ha, 0.05 to 0.1 ha, 0.1 to 1 ha, 1 to 10 ha, 10 to 50 ha, and above 50 ha, based on the size of the prediction mask at 10m resolution), treating any object overlap between the prediction and annotated ground-truth mask as a true positive (Supplementary Table 8). Based on these results, we removed reservoir detections smaller than 0.05 ha due to low accuracy (precision = 6.0% and recall = 2.9%) and larger than 50 ha due to lack of data (only 4 reservoirs from the annotated validation and test sets are larger than 50 ha) from all predictions and analysis.

III. Mapping across all 8.5 million km² of Brazil's land area

After model training and evaluation, we applied the model to all of Brazil—the 5th largest country in the world by land area at 8.5 million km^2—to create a wall-to-wall map of small reservoirs.

For the mapping, we used Sentinel-1 and Sentinel-2 cloud-free mosaics from 2021, the last year of full Sentinel-1 data availability before Sentinel-1B was decommissioned due to a power supply issue in 2022. The entire country was first divided into 640 x 640-pixel blocks (563,317 total), with adjacent blocks overlapping by 240 pixels to produce continuous 400 x 400-pixel outputs. Although the model was trained to output 500 x 500-pixel outputs, accuracy assessment and manual validation revealed that there was a higher rate of False Positives at the edges of the prediction tiles (validation precision for 500 x 500 was 80.7% vs. 83.6% for the center 400 x 400 of each prediction). After inference, all image blocks were mosaicked, using the mean of the output model scores in areas where multiple prediction tiles overlapped. The prediction threshold calculated during the training phase was applied (0.62) to create a binary reservoir map. Then all reservoirs with an area smaller than 0.05 ha (0.0005 km^2 or 5 pixels at 10m resolution) or greater than 50 ha (0.5 km^2) were removed.

In some cases, the model falsely identified segments of very large waterbodies (e.g., inlets or bays on lakes or large hydroelectric reservoirs) as small reservoirs. Since this was rare and only occurred for large, permanent waterbodies, we filtered out these false positives by removing any reservoirs that overlapped with a waterbody object larger than 50 ha in the ESRI/Garmin World Water Bodies dataset[76]. This removed 1,579 reservoir detections from the final maps (0.14%, Supplementary Table 10).

Since most detected reservoirs are small, their estimated area is sensitive to small errors in the reservoir prediction mask. To assess the impact of area errors and generate a range of uncertainty, we calculated reservoir areas after applying morphological erosion (shrinking each reservoir by 1-pixel around the perimeter) and dilation (growing each reservoir) using a 3x3 cross-shaped kernel (Supplementary Figure 3). This also affected the count of reservoirs, since it changed how many fell between the 0.05 ha minimum and 50 ha maximum size thresholds.

IV. Accuracy assessment and comparisons with other datasets

We evaluated the accuracy of the final model against the withheld test set of 263 annotated images. We calculated accuracy statistics on both a per-pixel (i.e., each pixel is evaluated as a true positive, true negative, false positive, or false negative) and per-object basis (i.e., each reservoir *object* is evaluated). For the object-based scores, a True Positive was considered any predicted reservoir object that intersected with a ground-truth object. In cases where multiple predictions overlapped with a single ground-truth object, only the largest prediction was considered a True Positive, and all others were classified as False Positives. We also calculated pixel-wise accuracy statistics in each biome (Supplementary Table 6) and object-based statistics for different size classes (Supplementary Table 8, same as previously discussed above in "II. Training MA-Net segmentation model").

To further assess model precision, we randomly selected 5,000 reservoir detections from the final prediction map to manually verify. We manually assessed each of these reservoirs using Google Satellite and ESRI World Imagery basemap data, categorizing them as "True Positive" and "False Positive". For manual verification, we used the same criteria as for annotating training data: (1) Is there a visible dam or other obstruction impounding the water? (2) Is there evidence of a stream path flowing into and/or out of the reservoir? For the "False Positive" results, we further described the type of error ("Natural Waterbody", "Non-Stream-Fed Impoundment", "Duplicate Detection", "Terrain Shadow", "Land", or "Fragment of Large Reservoir"). The results are shown in Supplementary Table 9.

Finally, we compared our results against eight different previous artificial reservoir datasets in Brazil (Supplementary Table 5). Where possible, we filtered out reservoirs larger than 50 ha from the other datasets before comparison. Of the eight, only four included data across all of Brazil: There are four existing reservoir datasets available for all of Brazil: the official waterbodies dataset from Brazil's National Water and Sanitation Agency (ANA)[40]; MapBiomas Agua's Landsat-based waterbodies dataset[42]; and a country-wide Cadastral Ambiental Rural dataset which we aggregated from state-level datasets available on SICAR[41]. We compared the total reservoir counts, areas, and agreement between our results and these datasets. We emphasize that previous mapping efforts have not specifically attempted to identify small reservoirs, and most used coarser resolution imagery. Our approach complements existing data products which focus on larger impoundments to provide comprehensive information on reservoirs of all sizes. Here we provide some discussion of the advantages and disadvantages of each.

Our total surface area is 43% higher and count is 557% higher compared to all sub-50 ha artificial waterbodies in the ANA waterbodies dataset, which was derived from a compilation of sources and is the most reliable data on waterbodies in Brazil to date. The ANA dataset is precise (i.e., low false positive rate), but most small reservoirs are absent (i.e., high false negative rate). Some regions appear much more detailed than others. The Mata Atlântica biome contains 76,496 reservoirs compared to our estimated 302,963, but the Amazon contains just 5,752 compared to our 273,444. It is most valuable for cases that demand minimal false positives and require information on reservoirs of varied sizes.

In Brazil, Global Dam Watch includes only 3824 reservoirs smaller than 50 ha. Global Dam Watch is a crucial central repository for large reservoir data, but small reservoirs are outside the focus of the dataset—according to the authors, the dataset is considered incomplete for reservoirs smaller than 10 km^2 and especially for reservoirs smaller than 0.1 km^2 [17]. With the goal of harmonizing the study of dams and their reservoirs, the full global dataset comprises 35,295 reservoirs—plus an additional 5850 barrier locations without reservoir polygons—and is an excellent resource for information on large-scale dams.

Compared to the MapBiomas Agua waterbodies product, derived from 30m-resolution Landsat data, our area is 44% higher and our count is 91% higher. The dataset includes five detailed waterbody classes (Natural, Mining, Reservoirs, Hydroelectric, and Aquaculture) but is limited in its detection of small reservoirs by Landsat's 30m resolution and prone to reservoir false positives in rivers and at the edges of large hydroelectric reservoirs. We recommend the dataset for applications that require specific classifications of waterbodies beyond natural and anthropogenic.

Finally, to create the unified CAR dataset, we downloaded the federal-unit hydrographic data from the national CAR database for all 26 states and the federal district (Brasília) using the SICAR package[41,77]. The state-level data are collected by each state's environmental ministry in order to meet the requirements of Brazil's forest law, which requires that the riparian areas around streams and artificial reservoirs be left as natural vegetation. The rural environmental registry process requires land-owners to register this information, and the state and municipalities must verify that the appropriate areas of each property are protected. In recent years, Brazil's Amazon Fund has invested tens of millions of dollars (US) into improving state-level CAR data by manually annotated forests, streams, artificial waterbodies, and more to help validate property-level registrations[78], for example. For some regions, this results in very high-quality reservoir data for even small reservoirs. For example, in Espírito Santo, 58,931 reservoirs smaller than 50 ha have been delineated—almost three-times how many we mapped—and most appear accurate. However, in other areas the data is missing, incomplete, and unreliable. Reservoirs that cross property boundaries are frequently fragmented and missing segments. Overall, we identified 71% more reservoirs with 35% more surface area. Nevertheless, the aggregated CAR dataset contains more sub-50 ha than any other existing reservoir database. Depending on the application and region of interest, the CAR dataset could be useful for researchers, but its regional inconsistencies limit is country-wide utility. We provide our aggregated CAR dataset for download[79].

V. Land-use/land-cover assessment

To assign reservoirs to land-use/land-cover (LULC) classes, we downloaded MapBiomas LULC Collection 10 data [44] for 2021. Six land-cover/land-use categories were analyzed: "Forest/Savanna" (MapBiomas classes 3, 4, 5, 6, 49), "Grass/Shrub" (classes 11, 12, 32, 29, 50), "Pasture" (class 15), "Crop" (classes 18, 19, 20, 35, 36, 39, 40, 41, 46, 47, 48, and 62), "Agricultural Mosaic" (class 21), and "Other" (all other classes). A 1-km buffer was calculated from the perimeter of each reservoir. Each reservoir was assigned to the class comprising the most pixels within its 1-km buffer, calculated using the "exactextract" package in Python[80]. Since reservoirs frequently sit in riparian vegetation within pasture and croplands, this method may overestimate how many reservoirs are associated with forest and underestimate the number associated with agriculture.

Assessing compliance with the Forest Code's Permanent Protected Area requirement[24] followed a similar process. We first created a 30 m buffer from the perimeter of all reservoirs larger than 1 ha in surface area (13.3% of our reservoir detections, or 149,804 total reservoirs; smaller reservoirs are exempt from the requirement). Then we calculated the fraction of all MapBiomas LULC classes within the buffer (excluding the original polygon), grouping the classes into three groups: "Natural" (classes 3, 4, 5, 6, 11, 12, 23, 29, 32, 49, 50, and 23), "Water" (classes 31 and 33), and "Other" (all other classes).

VI. Modeling reservoir counts per municipality

To better understand the distribution of reservoirs across the country, we modeled reservoir counts per municipality (n = 5,570) based on a range of social, economic, and environmental variables. We chose a generalized additive model (GAM) for its balance of power, flexibility, and explainability. We modeled reservoir counts as a negative binomial variable using a log link function and offset by the log of the municipality area. The GAM fitting and evaluation were performed in R using *mgcv*[81]**.**

We evaluated a wide range of socioeconomic and environmental variables: monthly precipitation[82]; cattle herd size[45]; total municipality area covered by natural vegetation, pasture, rice, corn, and soy (currently and change from 1985)[44]; soy, corn, and rice agricultural production by mass and value[83]; irrigated area[51]; total aquaculture production[84]; population[85]; gross domestic product (GDP) overall and agricultural-only[86]; and number of intersections between roads and streams within the municipality[52,87]. Missing data were filled with zeros. We eliminated variables with high concurvity (observed concurvity > 0.8) and non-significant Chi-Square tests of their fitted splines (α = 0.01). Notably, irrigated land area had a non-significant Chi-Square test. The agricultural production variables, including soy, corn, and rice yields, had high concurvity with the equivalent land-use/land-cover variables. In each case, we chose the variable that most increased the Akaike information criterion, which was LULC for soy and total production for rice.

In the end, we narrowed the list down to 11 total variables: municipality latitude and longitude (as a bivariate tensor product smooth), biome, cattle herd spatial density [45], mean monthly precipitation and standard deviation of monthly precipitation (bivariate tensor product smooth)[82], population density[85], agricultural-GDP per capita[86], % of municipality area dedicated to soy agriculture, total rice production in kilograms[44], total aquaculture production in kilograms[84], and % of land converted from natural land-covers (1985 to 2021; limited by the length of the Landsat record)[44]. The model diagnostics show that the residuals are approximately normally distributed around 0 and independent, other than a few outliers (Supplementary Figure 6). To evaluate the relative importance of each of these variables, we used the *gam.hp* package, which uses hierarchical partitioning to calculate the contribution of each variable to the overall explained deviance of the model[88] (Supplementary Table 11).

VII. Estimating evaporative water loss from reservoirs

To estimate the total evaporation from small reservoirs in Brazil, we use the following equation:

$$E_{res} = \sum_{i=1}^{N} A_i \times ET_{0,i} \times 365 \qquad (1)$$

Where E_{res} is the annual total evaporation from all reservoirs in m^3, N is the total number of reservoirs (1,126,861), A_i is the area of reservoir i in m^2, and $ET_{0,i}$ is the daily Penman-Monteith reference crop potential evapotranspiration in meters at the centroid of reservoir i, obtained from the Brazilian Daily Gridded Weather Dataset (BR-DWGD) available at 0.1° x 0.1° resolution[53,89]. We used reference potential evapotranspiration as a conservative best-guess evaporation rate since there is substantial uncertainty in the open water evaporation rates from small reservoirs, which are rarely the focus of *in situ* evaporation rate observations and may vary widely in turbidity, depth, and vegetation cover. Although better estimates can be attained with lake depth and/or local pan evaporation measurements[90], Penman-Monteith reference crop potential evapotranspiration is an established, conservative method for estimating open water evaporation[3,91–93], particularly for shallow water bodies since heat retention is a less important factor. For comparison, using the Penman open water evaporation equation[94] applied to the BR-DWGD resulted in 25% higher gross evaporation estimates but is likely an overestimate for small reservoirs which are frequently surrounded by trees which can break the wind and shade parts of the water surface.

To convert from total evaporation to *excess* evaporative water loss, we follow ANA's approach[39] by subtracting an estimate of the total baseline evapotranspiration from the reservoir surface areas if the reservoirs did *not* exist:

$$ET_{baseline} = \sum_{i=1}^{N} A_i \times ET_i^{baseline} \times 365 \qquad (2)$$

where $ET_i^{baseline}$ is the daily actual evapotranspiration at the reservoir centroid from the fourth generation Global Land Evaporation Amsterdam Model (GLEAM4) dataset, also at 0.1° x 0.1° [95]. While a rough estimate, ANA incorporates the hypothetical reservoir-absent evapotranspiration to the atmosphere to better represent the water balance impacts of the reservoirs. Taken together, total excess evaporative water loss (EWL_{res}) from the reservoirs is:

$$EWL_{res} = E_{res} - ET_{baseline} \qquad (3)$$

To account for reservoir surface area uncertainty, we calculate a range of evaporative water loss estimates using reservoir areas with morphological erosion and dilation applied (see "III. Mapping across all 8.5 million km^2 of Brazil's land area").

Data availability: The complete reservoir dataset is available at: https://doi.org/10.5281/zenodo.14927227[79]. The annotated training data, trained model weights, and manually validated reservoir detections are available at: https://doi.org/10.5281/zenodo.14927196[96].

Code Availability: All code used for training, modeling, and analysis is available at: https://doi.org/10.5281/zenodo.14933734[97].

References

1. Belletti, B. *et al.* More than one million barriers fragment Europe's rivers. *Nature* **588**, 436–441 (2020).
2. Sun, J. *et al.* Towards a comprehensive river barrier mapping solution to support environmental management. *Nat. Water* **3**, 38–48 (2025).
3. Lathuillière, M. J. *et al.* Cattle production in Southern Amazonia: implications for land and water management. *Environ. Res. Lett.* **14**, 114025 (2019).
4. Mady, B., Lehmann, P., Gorelick, S. M. & Or, D. Distribution of small seasonal reservoirs in semi-arid regions and associated evaporative losses. *Environ. Res. Commun.* **2**, 061002 (2020).

5. Chandesris, A., Van Looy, K., Diamond, J. S. & Souchon, Y. Small dams alter thermal regimes of downstream water. *Hydrol. Earth Syst. Sci.* **23**, 4509–4525 (2019).
6. Macedo, M. N. *et al.* Land-use-driven stream warming in southeastern Amazonia. *Philos. Trans. R. Soc. Lond. B. Biol. Sci.* **368**, 20120153 (2013).
7. Zaidel, P. A. *et al.* Impacts of small dams on stream temperature. *Ecol. Indic.* **120**, 106878 (2021).
8. Barbarossa, V. *et al.* Impacts of current and future large dams on the geographic range connectivity of freshwater fish worldwide. *Proc. Natl. Acad. Sci.* **117**, 3648–3655 (2020).
9. Fencl, J. S., Mather, M. E., Costigan, K. H. & Daniels, M. D. How Big of an Effect Do Small Dams Have? Using Geomorphological Footprints to Quantify Spatial Impact of Low-Head Dams and Identify Patterns of Across-Dam Variation. *PLOS ONE* **10**, e0141210 (2015).
10. Habets, F., Philippe, E., Martin, E., David, C. H. & Leseur, F. Small farm dams: impact on river flows and sustainability in a context of climate change. *Hydrol. Earth Syst. Sci.* **18**, 4207–4222 (2014).
11. Liu, Y. *et al.* Assessing Effects of Small Dams on Stream Flow and Water Quality in an Agricultural Watershed. *J. Hydrol. Eng.* **19**, 05014015 (2014).
12. Lange, K. *et al.* Basin-scale effects of small hydropower on biodiversity dynamics. *Front. Ecol. Environ.* **16**, 397–404 (2018).
13. Holgerson, M. A. & Raymond, P. A. Large contribution to inland water CO2 and CH4 emissions from very small ponds. *Nat. Geosci.* **9**, 222–226 (2016).
14. Ollivier, Q. R., Maher, D. T., Pitfield, C. & Macreadie, P. I. Punching above their weight: Large release of greenhouse gases from small agricultural dams. *Glob. Change Biol.* **25**, 721–732 (2019).
15. DelSontro, T., Beaulieu, J. J. & Downing, J. A. Greenhouse gas emissions from lakes and impoundments: Upscaling in the face of global change. *Limnol. Oceanogr. Lett.* **3**, 64–75 (2018).
16. Malerba, M. E., de Kluyver, T., Wright, N., Schuster, L. & Macreadie, P. I. Methane emissions from agricultural ponds are underestimated in national greenhouse gas inventories. *Commun. Earth Environ.* **3**, 306 (2022).
17. Lehner, B. *et al.* The Global Dam Watch database of river barrier and reservoir information for large-scale applications. *Sci. Data* **11**, 1069 (2024).
18. Wisser, D. *et al.* The significance of local water resources captured in small reservoirs for crop production – A global-scale analysis. *J. Hydrol.* **384**, 264–275 (2010).
19. Balaniuk, R., Isupova, O. & Reece, S. Mining and Tailings Dam Detection in Satellite Imagery Using Deep Learning. *Sensors* **20**, 6936 (2020).
20. Sousa, R. G. C., de Almeida Mereles, M., Siqueira-Souza, F. K., Hurd, L. E. & de Carvalho Freitas, C. E. Small dams for aquaculture negatively impact fish diversity in Amazonian streams. *Aquac. Environ. Interact.* **10**, 89–98 (2018).
21. Latrubesse, E. M. *et al.* Damming the rivers of the Amazon basin. *Nature* **546**, 363–369 (2017).
22. Congresso Nacional do Brasil. *Lei 9.433*. *9433* (1997).
23. Malveira, V. T. C., Araújo, J. C. de & Güntner, A. Hydrological Impact of a High-Density Reservoir Network in Semiarid Northeastern Brazil. *J. Hydrol. Eng.* **17**, 109–117 (2012).
24. Congresso Nacional do Brasil. *Lei 12.727*. *12727* (2012).
25. Amazon Fund. Projects. *Amazon Fund* https://www.amazonfund.gov.br/en/projetos (2025).
26. Khandelwal, A. *et al.* An approach for global monitoring of surface water extent variations in reservoirs using MODIS data. *Remote Sens. Environ.* **202**, 113–128 (2017).
27. Arvor, D. *et al.* Monitoring thirty years of small water reservoirs proliferation in the southern Brazilian Amazon with Landsat time series. *ISPRS J. Photogramm. Remote Sens.* **145**, 225–237 (2018).

28. Malerba, M. E., Wright, N. & Macreadie, P. I. A Continental-Scale Assessment of Density, Size, Distribution and Historical Trends of Farm Dams Using Deep Learning Convolutional Neural Networks. *Remote Sens.* **13**, 319 (2021).
29. Sun, J. *et al.* Convolutional Neural Networks Facilitate River Barrier Detection and Evidence Severe Habitat Fragmentation in the Mekong River Biodiversity Hotspot. *Water Resour. Res.* **60**, e2022WR034375 (2024).
30. Buchanan, B. P. *et al.* A machine learning approach to identify barriers in stream networks demonstrates high prevalence of unmapped riverine dams. *J. Environ. Manage.* **302**, 113952 (2022).
31. Jones, S. K. *et al.* Big Data and Multiple Methods for Mapping Small Reservoirs: Comparing Accuracies for Applications in Agricultural Landscapes. *Remote Sens.* **9**, 1307 (2017).
32. Fan, T., Wang, G., Li, Y. & Wang, H. MA-Net: A Multi-Scale Attention Network for Liver and Tumor Segmentation. *IEEE Access* **8**, 179656–179665 (2020).
33. Zhang, Y. *et al.* MU-Net: Embedding MixFormer into Unet to Extract Water Bodies from Remote Sensing Images. *Remote Sens.* **15**, 3559 (2023).
34. Dong, R., Pan, X. & Li, F. DenseU-Net-Based Semantic Segmentation of Small Objects in Urban Remote Sensing Images. *IEEE Access* **7**, 65347–65356 (2019).
35. Feng, Y., Jiang, J., Xu, H. & Zheng, J. Change Detection on Remote Sensing Images Using Dual-Branch Multilevel Intertemporal Network. *IEEE Trans. Geosci. Remote Sens.* **61**, 1–15 (2023).
36. Zi, Y., Ding, H., Xie, F., Jiang, Z. & Song, X. Wavelet Integrated Convolutional Neural Network for Thin Cloud Removal in Remote Sensing Images. *Remote Sens.* **15**, 781 (2023).
37. Guo, M., Liu, H., Xu, Y. & Huang, Y. Building Extraction Based on U-Net with an Attention Block and Multiple Losses. *Remote Sens.* **12**, 1400 (2020).
38. Jing, Y., Ren, Y., Liu, Y., Wang, D. & Yu, L. Dam Extraction from High-Resolution Satellite Images Combined with Location Based on Deep Transfer Learning and Post-Segmentation with an Improved MBI. *Remote Sens.* **14**, 4049 (2022).
39. ANA. *Manual de Usos Consuntivos da Água no Brasil - 2ª Edição*. 109 (2024).
40. ANA. *Atualização Da Base de Dados Nacional de Referência de Massas d'Água*. (2020).
41. Ministério do Meio Ambiente e Mudança do Clima. Base de Downloads. *Sistema de Cadastro Ambiental Rural* https://consultapublica.car.gov.br/publico/estados/downloads (2025).
42. MapBiomas. Mapping of the Water Surface of Brazil - Collection 4. (2025).
43. ESRI. World Imagery [basemap]. (2025).
44. MapBiomas. Collection 10 of the annual series of Maps of Land Cover and Land Use of Brazil. https://brasil.mapbiomas.org (2025).
45. IBGE. Tabela 3939: Efetivo dos rebanhos, por tipo de rebanho. *Instituto Brasileiro de Geografia e Estatística* https://sidra.ibge.gov.br/tabela/3939.
46. Caballero, C. B., Biggs, T. W., Vergopolan, N., West, T. A. P. & Ruhoff, A. Transformation of Brazil's biomes: The dynamics and fate of agriculture and pasture expansion into native vegetation. *Sci. Total Environ.* **896**, 166323 (2023).
47. Cerecetto, V. *et al.* Pasture-crop rotations modulate the soil and rhizosphere microbiota and preserve soil structure supporting oat cultivation in the Pampa biome. *Soil Biol. Biochem.* **195**, 109451 (2024).
48. Song, X.-P. *et al.* Massive soybean expansion in South America since 2000 and implications for conservation. *Nat. Sustain.* **4**, 784–792 (2021).
49. Cavalcante, L., Dewulf, A. & Van Oel, P. Fighting against, and coping with, drought in Brazil: two policy paradigms intertwined. *Reg. Environ. Change* **22**, 111 (2022).
50. IBGE. Biomas e Sistema Costeiro-Marinho do Brasil. https://www.ibge.gov.br/geociencias/informacoes-ambientais/vegetacao/15842-biomas.html?edicao=25799&t=acesso-ao-produto (2019).
51. ANA. *Atlas Irrigação - 2ª Edição*. 66 (2021).

52. ANA. Base Hidrográfica Ottocodificada 1:250.000 (BHO250). *Catálogo de Metadados da ANA* https://metadados.snirh.gov.br/geonetwork/srv/eng/catalog.search#/metadata/0f57c8a0-6a0f-4283-8ce3-114ba904b9fe (2018).
53. Xavier, A. C., Scanlon, B. R., King, C. W. & Alves, A. I. New improved Brazilian daily weather gridded data (1961–2020). *Int. J. Climatol.* **42**, 8390–8404 (2022).
54. Coe, M. T., Costa, M. H. & Soares-Filho, B. S. The influence of historical and potential future deforestation on the stream flow of the Amazon River – Land surface processes and atmospheric feedbacks. *J. Hydrol.* **369**, 165–174 (2009).
55. Coe, M. T., Latrubesse, E. M., Ferreira, M. E. & Amsler, M. L. The effects of deforestation and climate variability on the streamflow of the Araguaia River, Brazil. *Biogeochemistry* **105**, 119–131 (2011).
56. Levy, M. C., Lopes, A. V., Cohn, A., Larsen, L. G. & Thompson, S. E. Land Use Change Increases Streamflow Across the Arc of Deforestation in Brazil. *Geophys. Res. Lett.* **45**, 3520–3530 (2018).
57. Chagas, V. B. P., Chaffe, P. L. B. & Blöschl, G. Climate and land management accelerate the Brazilian water cycle. *Nat. Commun.* **13**, 5136 (2022).
58. Ballarin, A. S. *et al.* Brazilian Water Security Threatened by Climate Change and Human Behavior. *Water Resour. Res.* **59**, e2023WR034914 (2023).
59. Dosskey, M. G. *et al.* The Role of Riparian Vegetation in Protecting and Improving Chemical Water Quality in Streams. *JAWRA J. Am. Water Resour. Assoc.* **46**, 261–277 (2010).
60. Souza, A. L. T. de, Fonseca, D. G., Libório, R. A. & Tanaka, M. O. Influence of riparian vegetation and forest structure on the water quality of rural low-order streams in SE Brazil. *For. Ecol. Manag.* **298**, 12–18 (2013).
61. Rodrigues, I. S., Costa, C. A. G., Raabe, A., Medeiros, P. H. A. & de Araújo, J. C. Evaporation in Brazilian dryland reservoirs: Spatial variability and impact of riparian vegetation. *Sci. Total Environ.* **797**, 149059 (2021).
62. Heinzel, C., Fink, M. & Höllermann, B. The potential of unused small-scale water reservoirs for climate change adaptation: A model- and scenario based analysis of a local water reservoir system in Thuringia, Germany. *Front. Water* **4**, (2022).
63. Gorelick, N. *et al.* Google Earth Engine: Planetary-scale geospatial analysis for everyone. *Remote Sens. Environ.* **202**, 18–27 (2017).
64. Pekel, J.-F., Cottam, A., Gorelick, N. & Belward, A. S. High-resolution mapping of global surface water and its long-term changes. *Nature* **540**, 418–422 (2016).
65. Pasquarella, G. All Clear with Cloud Score+. *Medium* https://medium.com/google-earth/all-clear-with-cloud-score-bd6ee2e2235e (2024).
66. Labelbox. https://labelbox.com (2025).
67. McFeeters, S. K. The use of the Normalized Difference Water Index (NDWI) in the delineation of open water features. *Int. J. Remote Sens.* **17**, 1425–1432 (1996).
68. Ronneberger, O., Fischer, P. & Brox, T. U-net: Convolutional networks for biomedical image segmentation. in *International Conference on Medical image computing and computer-assisted intervention* 234–241 (Springer, 2015).
69. Xie, E. *et al.* SegFormer: Simple and Efficient Design for Semantic Segmentation with Transformers. Preprint at https://doi.org/10.48550/arXiv.2105.15203 (2021).
70. Iakubovskii, P. Segmentation Models Pytorch. *GitHub repository* GitHub (2019).
71. He, K., Zhang, X., Ren, S. & Sun, J. Deep Residual Learning for Image Recognition. in *2016 IEEE Conference on Computer Vision and Pattern Recognition (CVPR)* 770–778 (IEEE, Las Vegas, NV, USA, 2016). doi:10.1109/CVPR.2016.90.
72. Kingma, D. P. & Ba, J. Adam: A Method for Stochastic Optimization. Preprint at https://doi.org/10.48550/arXiv.1412.6980 (2017).
73. Loshchilov, I. & Hutter, F. Decoupled Weight Decay Regularization. Preprint at https://doi.org/10.48550/arXiv.1711.05101 (2019).

74. Gao, B. NDWI—A normalized difference water index for remote sensing of vegetation liquid water from space. *Remote Sens. Environ.* **58**, 257–266 (1996).
75. Xu, H. Modification of normalised difference water index (NDWI) to enhance open water features in remotely sensed imagery. *Int. J. Remote Sens.* **27**, 3025–3033 (2006).
76. ESRI & Garmin. World Water Bodies. https://hub.arcgis.com/content/e750071279bf450cbd510454a80f2e63 (2024).
77. Urbano, G. SICAR Package. GitHub (2025).
78. Amazon Fund. Environmental Regularization. *Amazon Fund* https://www.amazonfund.gov.br/en/projeto/Environmental-Regularization/.
79. Solvik, K. *et al.* Map of small reservoirs in Brazil in 2021, from 'Mapping one million small reservoirs in Brazil highlights widespread environmental and policy implications'. Zenodo https://doi.org/10.5281/zenodo.20072849 (2026).
80. Baston, D. exactextract. GitHub (2025).
81. Wood, S. N., Pya, N. & Säfken, B. Smoothing Parameter and Model Selection for General Smooth Models. *J. Am. Stat. Assoc.* **111**, 1548–1563 (2016).
82. Raphael, S. Climatological normals and indicators for Brazilian municipalities. Zenodo https://doi.org/10.5281/zenodo.15519719 (2025).
83. IBGE. Tabela 5457: Área plantada ou destinada à colheita, área colhida, quantidade produzida, rendimento médio e valor da produção das lavouras temporárias e permanentes. *Instituto Brasileiro de Geografia e Estatística* https://sidra.ibge.gov.br/tabela/5457.
84. IBGE. Tabela 3940: Produção da aquicultura, por tipo de produto. *Instituto Brasileiro de Geografia e Estatística* https://sidra.ibge.gov.br/tabela/3940.
85. IBGE. Tabela 6579: População residente estimada. *Instituto Brasileiro de Geografia e Estatística* https://sidra.ibge.gov.br/tabela/6579.
86. IBGE. Produto Interno Bruto dos Municípios. *Instituto Brasileiro de Geografia e Estatística* https://www.ibge.gov.br/estatisticas/economicas/contas-nacionais/9088-produto-interno-bruto-dos-municipios.html?lang=pt-BR&t=o-que-e.
87. IBGE. Continuous cartographic bases - Brazil | IBGE. *IBGE* https://www.ibge.gov.br/en/geosciences/maps/continuous-cartographic-bases/18067-continuous-cartographic-bases-brazil.html (2025).
88. Lai, J., Tang, J., Li, T., Zhang, A. & Mao, L. Evaluating the relative importance of predictors in Generalized Additive Models using the *gam.hp* R package. *Plant Divers.* **46**, 542–546 (2024).
89. Allen, R. G., Pereira, L. S., Raes, D., Smith, M., & others. Crop evapotranspiration-Guidelines for computing crop water requirements-FAO Irrigation and drainage paper 56. *Fao Rome* **300**, D05109 (1998).
90. McMahon, T. A., Peel, M. C., Lowe, L., Srikanthan, R. & McVicar, T. R. Estimating actual, potential, reference crop and pan evaporation using standard meteorological data: a pragmatic synthesis. *Hydrol. Earth Syst. Sci.* **17**, 1331–1363 (2013).
91. Kohli, A. & Frenken, K. *Evaporation from Artificial Lakes and Reservoirs*. (2015).
92. Craig, I. P. Comparison of precise water depth measurements on agricultural storages with open water evaporation estimates. *Agric. Water Manag.* **85**, 193–200 (2006).
93. Dlouhá, D., Dubovský, V. & Pospíšil, L. Optimal Calibration of Evaporation Models against Penman–Monteith Equation. *Water* **13**, 1484 (2021).
94. Penman, H. L. Natural evaporation from open water, bare soil and grass. *Proc. R. Soc. Lond. Math. Phys. Sci.* **193**, 120–145 (1948).
95. Miralles, D. G. *et al.* GLEAM4: global land evaporation and soil moisture dataset at 0.1° resolution from 1980 to near present. *Sci. Data* **12**, 416 (2025).
96. Solvik, K. *et al.* Model weights and training, validation, and test set images and masks for 'Mapping one million small reservoirs in Brazil highlights widespread environmental and policy implications'. Zenodo https://doi.org/10.5281/zenodo.18199630 (2026).

97. Solvik, K. kysolvik/reservoir-id-smp: v0.3.3. Zenodo https://doi.org/10.5281/zenodo.21724891 (2026).
98. Souza, C. M., Kirchhoff, F. T., Oliveira, B. C., Ribeiro, J. G. & Sales, M. H. Long-Term Annual Surface Water Change in the Brazilian Amazon Biome: Potential Links with Deforestation, Infrastructure Development and Climate Change. *Water* **11**, 566 (2019).

Acknowledgments: Tomas Carvalho, Vivian Ribeiro, Nanxu Su, and Ylva Ran for their help annotating training data. We thank the anonymous reviewers for their valuable feedback and suggestions. This project was supported by grants from the National Aeronautics and Space Administration (80NSSC23K1616 and NNX16AI55G) and the National Science Foundation (1950832 and DBI-2153040).

Author contributions:

Conceptualization: KS, YT, MNM

Methodology: KS, MJL, ADC, MTC, MNM

Visualization: KS, CS, MNM

Funding acquisition: KS, YT, MNM

Supervision: YT, JKB, MNM

Writing – original draft: KS, MNM

Writing – review & editing: YT, JKB, MJL, THF, MTC, CMS, MNM

Competing interests: Authors declare that they have no competing interests.

Supplementary Information

Supplementary Figures 1 to 6

Supplementary Tables 1 to 11

Supplementary Information

Mapping one million small reservoirs in Brazil highlights widespread environmental and policy implications

Kylen Solvik, Yaffa Truelove, Jennifer K. Balch, Michael J. Lathuillière, Thiago H. Fontenelle, Andréa D. de Almeida Castanho, Michael T. Coe, Christina Shintani, Carlos M. Souza Jr., Marcia N. Macedo

Corresponding author: kylen.solvik@columbia.edu

The PDF file includes:

Supplementary Figures 1 to 6
Supplementary Tables 1 to 11

Supplementary Figure 1.

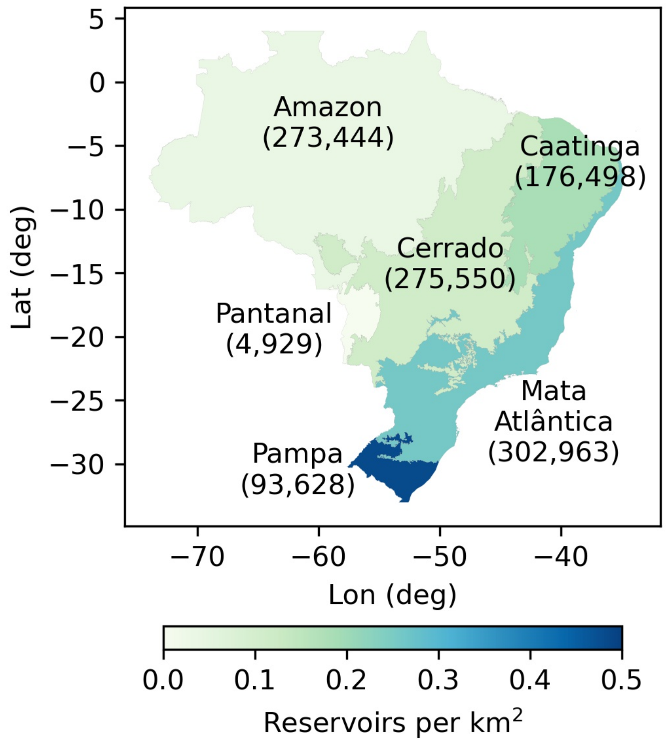

Reservoir count per km^2 land area in each Brazilian biome, with total counts in parenthesis.

Supplementary Figure 2.

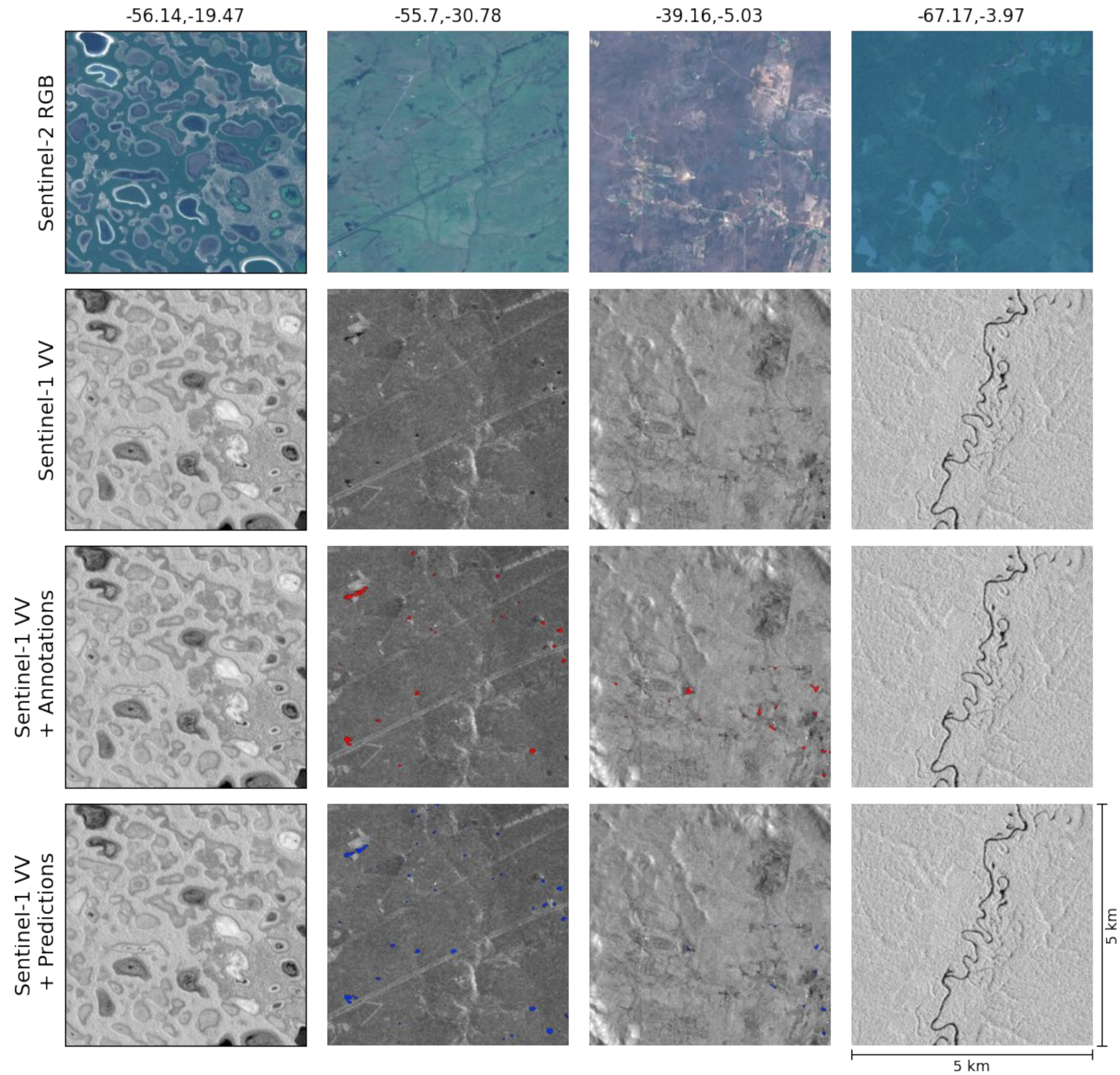

Examples of 5 km x 5 km subsets of cloud-free Sentinel satellite mosaics over Brazil used for training and prediction, with annotations and final predictions. Examples taken from validation set. *Top:* True color composite of Sentinel-2 using Bands 4 (Red), 3 (Green), and 2 (Blue). *2nd Row:* Sentinel-1 in VV polarization mode. *3rd Row:* Sentinel-1 with manual reservoir annotations. Note that the first and last examples contain natural water bodies but no reservoirs. *Bottom:* Sentinel-1 with final predictions.

Supplementary Figure 3.

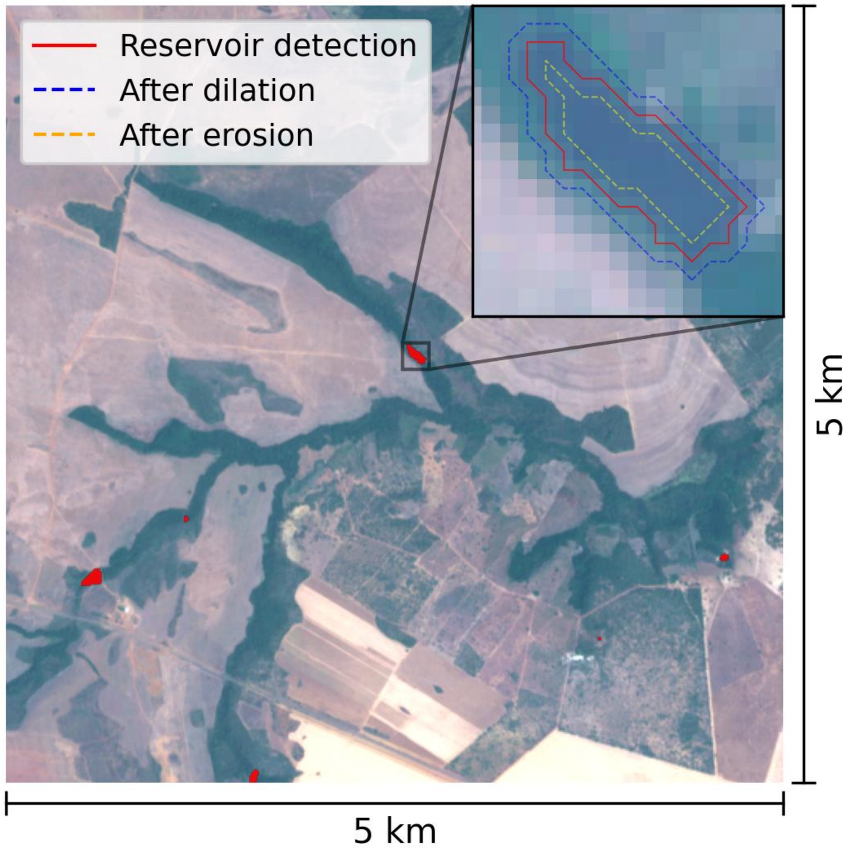

The MA-Net accurately delineates full reservoir outlines in Sentinel imagery. A detailed example of reservoir prediction from Mato Grosso, Brazil, displayed against Sentinel-2 true color imagery.

Supplementary Figure 4.

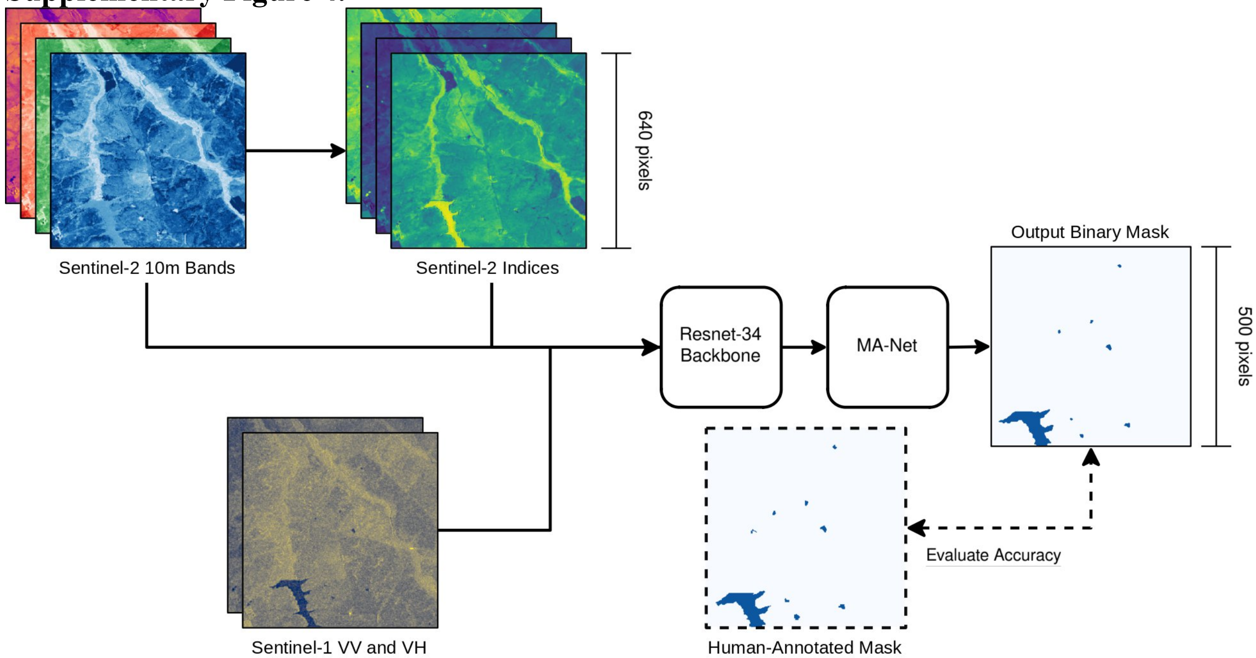

Flow chart of training and prediction process. A total of 10 bands are used as inputs, each 640 x 640 pixels. The output is a 500 x 500-pixel binary mask, with 1 representing a reservoir pixel and 0 representing land and non-reservoir water. During training, the human-annotated masks are used to fit the model.

Supplementary Figure 5.

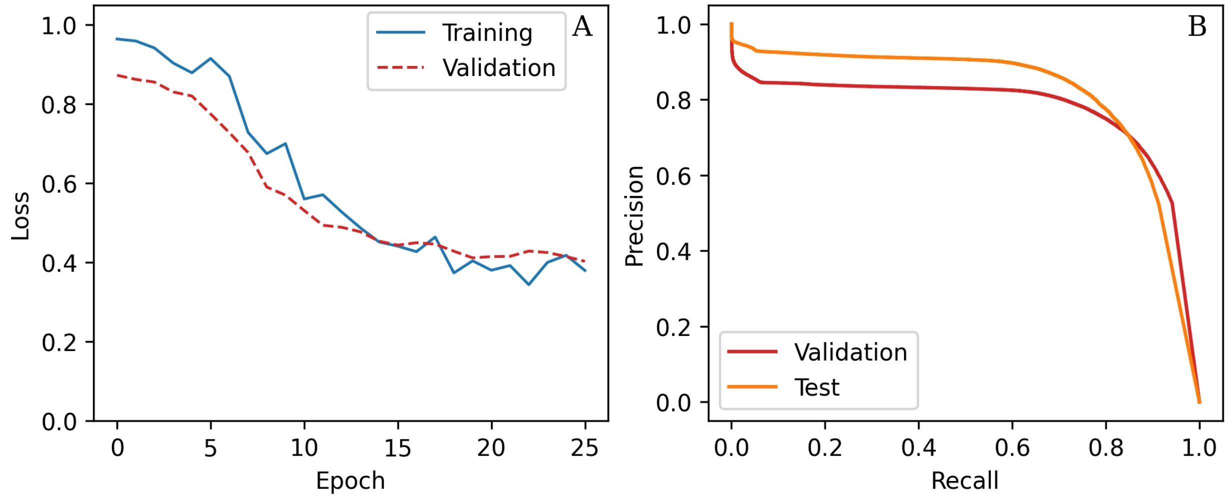

Model accuracy metrics during training and evaluation. (**A**) Progression of Training- and Validation-set Dice loss during training. (**B**) Precision-Recall curves for Validation and Test sets.

Supplementary Figure 6.

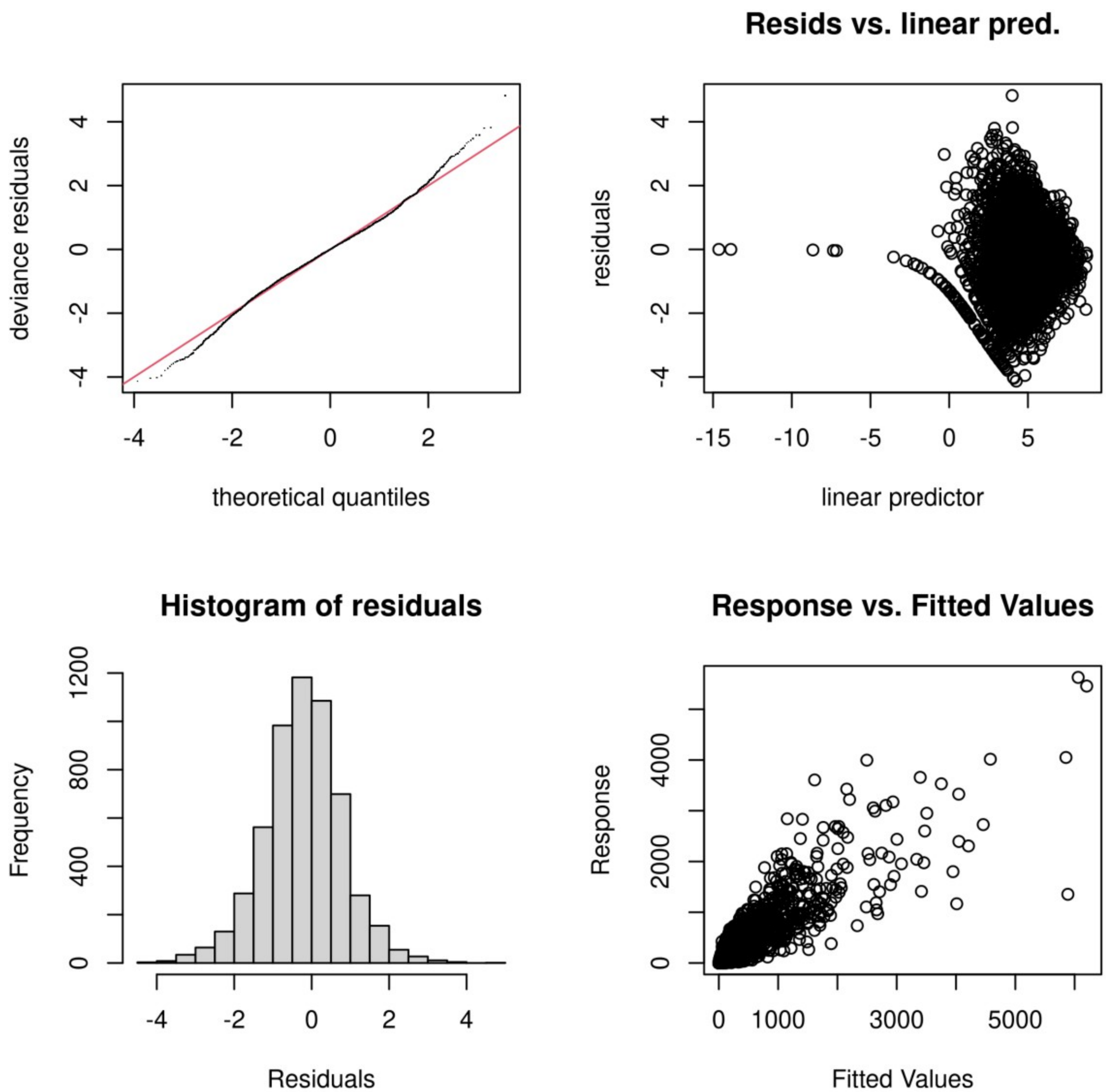

Diagnostic plots for residuals of generalized additive model of per-municipality reservoir counts.

Supplementary Table 1.
Reservoir statistics by biome. The maximum value in each column is shown in bold.

Biome	*Count*	*Total Area (km^2)*	*Median Area (ha)*	*Density (#/km^2)*	*MapBiomas (MB) Water Bodies Total Count* [42]	*Reservoir Count as % of MB*	*MB Water Bodies Total Area (km^2)*	*Reservoir Area as % of MB*	*Global Dam Watch Largest Reservoir Area (km^2)* [17]
Amazônia	273,444	1326	0.17	0.06	**680,929**	40.2	**1,040,822**	1.3%	2339 (Tucuruí)
Caatinga	176,498	1496	0.22	0.20	142,034	**124.3%**	77,236	**19.4%**	**2604** (Sobradinho)
Cerrado	275,550	**1797**	0.22	0.14	275,047	100.2	131,718	13.7%	926 (Furnas)
Mata Atlântica	**302,963**	1636	0.23	0.27	278,884	108.6	185,270	8.8%	1202 (Porto Primavera)
Pampa	93,628	1324	**0.27**	**0.48**	60,556	154.6	176,999	7.5%	192 (Passo Real)
Pantanal	4,929	17	0.13	0.03	28,166	17.5	6,091	0.3%	55 (unnamed)

Supplementary Table 2.

Reservoir statistics by state. The maximum value in each column is shown in bold.

State	*Count*	*Total Area (km^2)*	*Median Area (ha)*	*Density (#/km^2)*	*CAR Count* [41]	*CAR Area (km^2)*
Rio Grande do Sul	**138,558**	**1541**	0.25	**0.52**	25,900	489
Goiás	97,405	677	0.23	0.29	68,457	536
Minas Gerais	91,793	528	0.23	0.16	83,939	384
Pará	85,507	352	0.15	0.07	13,600	117
Mato Grosso	80,551	513	0.21	0.09	**136,176**	546
Maranhão	72,295	256	0.16	0.22	7,249	60
Bahia	65,176	297	0.17	0.12	11	0
São Paulo	64,702	492	0.29	0.26	45,543	222
Ceará	59,156	667	0.32	0.40	57,118	**1391**
Rondônia	54,251	268	0.19	0.23	22,057	137
Paraná	38,039	198	0.22	0.19	20,222	99
Mato Grosso do Sul	37,738	226	0.19	0.11	24,861	165
Tocantins	36,744	224	0.19	0.13	25,513	249
Santa Catarina	32,414	160	0.23	0.34	13,385	54
Pernambuco	29,918	167	0.19	0.30	6,985	104
Paraíba	26,610	274	0.26	0.47	21,315	336
Acre	24,277	97	0.18	0.15	5,385	28
Espírito Santo	21,391	133	0.27	0.46	58,931	255
Rio Grande do Norte	14,804	214	**0.38**	0.28	13,527	347
Piauí	13,487	73	0.21	0.05	1,871	38
Alagoas	10,369	49	0.16	0.37	2,194	18
Sergipe	10,130	29	0.14	0.46	1,067	5
Rio de Janeiro	9,216	45	0.22	0.21	2,262	9
Roraima	6,214	82	0.33	0.03	576	24
Amazonas	4,996	24	0.19	0.00	2,041	21
Distrito Federal	878	6	0.24	0.15	395	4
Amapá	405	3	0.28	0.00	57	4

Supplementary Table 3.

Reservoir statistics by macroregion. The maximum value of each column is shown in bold.

Region	*Count*	*Total Area (km^2)*	*Median Area (ha)*	*Density (#/km^2)*
Nordeste	**301,946**	**2025**	0.20	0.19
Centro-Oeste	216,574	1422	0.22	0.13
Norte	212,391	1051	0.17	0.06
Sul	209,011	1899	0.24	**0.37**
Sudeste	187,102	1198	**0.25**	0.20

Supplementary Table 4.

Reservoir statistics by major hydrographic region. The maximum value of each column is shown in bold.

Name	*Count*	*Total Area (km^2)*	*Median Area (ha)*	*Density (#/km^2)*	*% in headwater sub-basins**
Paraná	**190,032**	**1343**	**0.27**	0.22	71.4%
Tocantins-Araguaia	168,716	899	0.18	0.18	85.0%
Amazônica	164,454	933	0.20	0.04	69.2%
Atlântico Nordeste Oriental	118,240	1212	**0.27**	0.42	76.2%
Uruguai	88,695	1015	0.25	**0.51**	83.1%
Atlântico Leste	82,656	391	0.18	0.21	79.6%
Atlântico Sul	79,428	671	0.24	0.43	80.4%
Atlântico Nordeste Ocidental	67,915	253	0.16	0.25	**89.5%**
São Francisco	59,906	354	0.19	0.09	75.5%
Atlântico Sudeste	48,880	226	0.22	0.23	86.5%
Paraguai	39,772	170	0.16	0.11	74.2%
Parnaíba	18,317	129	0.22	0.05	77.8%

**Strahler stream order of 1-3*

Supplementary Table 5.
Reservoir area and count (this study) compared with previous datasets.

Comparison Source	Region Overlap	Year	Method	This Study Area (km^2)	Comp. Area (km^2)	This Study Count	Comp. Count	Shared Count
ANA[40]	Brazil	2019	Manual/Aggregate	7597 (5072 – 10,770)	5299	1,126,861 (725,267 – 1,280,671)	171,678	130,940
MapBiomas Agua[42]	Brazil	2021	Random Forest (Landsat)	7597 (5072 – 10,770)	5263	1,126,861 (725,267 – 1,280,671)	589,577	387,242
CAR[41]	Brazil	2025	Manual/Aggregate	7597 (5072 – 10,770)	5643	1,126,861 (725,267 – 1,280,671)	660,686	245,356
Lehner et al.[17]	Brazil	2024	Aggregate	7597 (5072 – 10,770)	709	1,126,861 (725,267 – 1,280,671)	3824	3259
Macedo et al.[6]	Upper Xingu basin	2007	eCognition (Aster)	110 (76 – 150)	188	10,789 (8297 – 11,723)	9977	5351
Souza et al.[98]*	Amazon biome	2017	Random Forest (Landsat)	1326 (762 – 2028)	1223	273,444 (156,399 – 319,460)	>50,000	N/A
Arvor et al.[27]*	Sorriso muni.	2015	Temporal (Landsat)	11.3 (8.8 –14.7)	17.1	701 (595 – 743)	522	N/A
Lathuillière et al.[3]	Mato Grosso state	2014	Random Forest (Landsat)	513	593	80,553	31,985	18,937

**Not filtered to reservoirs smaller than 50 ha.*

Supplementary Table 6.
Test-set accuracy by biome. Unless otherwise specified, metrics are computed on a pixel-wise basis.

Biome	*Train Count (images)*	*Test Count (images)*	*Annotated Reservoir Pixels (test set)*	*Precision*	*Recall*	*F1-Score*	*# of Detections Manually Checked*	*Manually Validated Precision (object-based)*
Amazônia	422	124	11,048	80.0%	66.8%	72.7%	1221	76.1%
Caatinga	82	15	1569	82.5%	62.7%	71.2%	792	70.3%
Cerrado	302	84	22,388	74.0%	82.5%	77.9%	1207	68.6%
Mata Atlântica	105	32	5532	58.5%	59.6%	59.0%	1334	52.7%
Pampa	21	2	15,991	90.9%	92.2%	91.5%	428	65.7%
Pantanal	46	6	19	3.3%	5.3%	4.1%	18	38.9%
All	978	263	56,547	78.4%	79.2%	78.8%	5000	66.1%

Supplementary Table 7.
Pixel-wise accuracy statistics for evaluated model architectures (max in each column bolded)

			Validation			Test		
Model	**Tuned Prediction Threshold**	**Epochs**	**F1**	**Precision**	**Recall**	**F1**	**Precision**	**Recall**
U-Net	0.70	18	77.2	**81.1**	73.8	67.6	59.8	77.8
MA-Net	0.62	20	**77.4**	80.7	**74.4**	**78.7**	**78.3**	**79.2**
Segformer	0.67	15	73.8	75.1	72.6	71.1	67.8	74.7

Supplementary Table 8.
Accuracy by size (object-based)

Set	*Size (ha)*	*True Count*	*Predicted Count*	*Precision*	*Recall*
Train	*< 0.05**	*443*	*252*	*31.3%*	*7.7%*
	0.05 to 0.1	590	344	55.5%	32.3%
	0.1 to 1	1383	1287	75.1%	74.0%
	1 to 10	273	290	91.4%	93.0%
	10 to 50	27	26	100.0%	92.6%
	*> 50**	4	3	*100.0%*	*75.0%*
	All	**2273**	**1947**	**74.4%**	**65.7%**
Validation	*< 0.05**	*115*	*87*	*36.8%*	*2.6%*
	0.05 to 0.1	155	101	46.5%	28.4%
	0.1 to 1	401	387	72.6%	76.3%
	1 to 10	80	84	83.3%	95.0%
	10 to 50	8	6	100.0%	87.5%
	*> 50**	*2*	*1*	*100.0%*	*50.0%*
	All	**644**	**578**	**69.9%**	**67.2%**
Test	*< 0.05**	*155*	*92*	*51.1%*	*9.0%*
	0.05 to 0.1	245	124	62.9%	28.6%
	0.1 to 1	510	399	79.4%	72.0%
	1 to 10	78	92	89.1%	96.2%
	10 to 50	3	5	60.0%	66.0%
	*> 50**	*2*	*1*	*100.0%*	*50.0%*
	All	**836**	**620**	**77.4%**	**61.4%**

*****_Removed from "All" and from final predictions._

Supplementary Table 9.
Manual validation results for 5000 randomly selected reservoir predictions

Label	*Error Type*	*Count*	*Percentage*
True Positive	True Positive	3305	66.10%
False Positive	Natural Waterbody	375	7.50%
	Non-Stream-Fed Impoundment	1226	24.52%
	Duplicate Detection	67	1.34%
	Land	15	0.30%
	Shadow	10	0.20%
	Fragment of large (>50 ha) reservoir	2	0.04%

Supplementary Table 10.
Reservoir counts during post-processing

Stage	*Reservoir Count*	*Total Area (km^2)*
Raw predictions	1,311,248	8252
Filter to < 50 ha	1,310,534	7716
Filter to >= 5 ha	1,128,440	7671
Remove known natural water bodies	1,126,861	7597

Supplementary Table 11.
Municipality reservoir count GAM predictors ranked by contribution to total explained deviance.

Variable	*Unique*	*Avg. Shared*	*Total (Unique – Avg. Shared)*	*Percentage Contribution*
Cattle Herd Size per km^2	0.1236	0.0563	0.1799	32.8%
Coordinates	0.0700	0.0503	0.1203	21.9%
Annual mean and standard deviation of monthly precipitation	0.0410	0.0753	0.1163	21.2%
Population Density	0.0094	0.0237	0.0331	6.0%
Road-River Crossings per km^2	0.0134	0.0171	0.0305	5.6%
Biome	0.0031	0.0179	0.0210	3.8%
% Land Cleared since 1985	0.0127	0.0078	0.0205	3.7%
% Land Dedicated to Soy Agriculture	0.0137	-0.0040	0.0097	1.8%
Agricultural GDP per capita	0.0045	0.0028	0.0073	1.3%
Aquaculture Production (kg/km^2)	0.0018	0.0052	0.0070	1.3%
Rice production (kg/km^2)	0.0025	0.0006	0.0031	0.6%